

1 THEMED ISSUE: Anatomy of Rifting: Tectonics and Magmatism in Continental Rifts,
2 Oceanic Spreading Centers, and Transforms
3 Research Paper
4 Peace et al.

5 The asymmetric margins of the Labrador Sea
6 GEOSPHERE, v. 12, no. X, p. XXX–XXX
7 doi:10.1130/GES01341.1

8 16 figures; 5 tables; 3 supplemental files

9 CORRESPONDENCE: a.l.peace@durham.ac.uk

10 CITATION: Peace, A., McCaffrey, K., Imber, J., Phethean, J., Nowell, G., Gerdes, K., and
11 Dempsey, E., 2016, An evaluation of Mesozoic rift-related magmatism on the margins of the
12 Labrador Sea: Implications for rifting and passive margin asymmetry: Geosphere, v. 12, no.
13 X, p. XXX–XXX, doi:10.1130/GES01341.1.

14 Received 9 April 2016

15 Revision received 3 August 2016

16 Accepted 24 August 2016

17 Published online XX Month 2016

18 ¹Supplementary Materials 1. Detailed descriptions of all samples mentioned in the
19 manuscript. Please visit <http://dx.doi.org/10.1130/GES01341.S1> or the full-text article on
20 www.gsapubs.org to view Supplementary Materials 1.

21 ²Supplementary Materials 2. Sample locations and coordinate systems. Please visit
22 <http://dx.doi.org/10.1130/GES01341.S2> or the full-text article on www.gsapubs.org to view
23 Supplementary Materials 2.

24 ³Supplementary Materials 3. X-Ray Fluorescence analysis and other datasets. Please visit
25 <http://dx.doi.org/10.1130/GES01341.S3> or the full-text article on www.gsapubs.org to view
26 Supplementary Materials 3.

27 **An evaluation of Mesozoic rift-related magmatism on the**
28 **margins of the Labrador Sea: Implications for rifting and**
29 **passive margin asymmetry**

30 **Alex Peace¹, Ken McCaffrey¹, Jonathan Imber¹, Jordan Phethean¹, Geoff Nowell¹,**
31 **Keith Gerdes², and Edward Dempsey¹**

32 ¹*Department of Earth Sciences, Science Labs, Durham University, Elvet Hill, Durham DH1*
33 *3LE, UK*

34 ²*Shell International, 40 Bank Street, London E14 5NR, UK*

35 **ABSTRACT**

36 The Labrador Sea is a small (~900 km wide) ocean basin separating southwest
37 Greenland from Labrador, Canada. It opened following a series of rifting events that began as
38 early as the Late Triassic or Jurassic, culminating in a brief period of seafloor spreading
39 commencing by polarity chron 27 (C27; Danian) and ending by C13 (Eocene-Oligocene
40 boundary). Rift-related magmatism has been documented on both conjugate margins of the
41 Labrador Sea. In southwest Greenland this magmatism formed a major coast-parallel dike
42 swarm as well as other smaller dikes and intrusions. Evidence for rift-related magmatism on

43 the conjugate Labrador margin is limited to igneous lithologies found in deep offshore
44 exploration wells, mostly belonging to the Alexis Formation, along with a postulated Early
45 Cretaceous nephelinite dike swarm (ca. 142 Ma) that crops out onshore, near Makkovik,
46 Labrador. Our field observations of this Early Cretaceous nephelinite suite lead us to
47 conclude that the early rift-related magmatism exposed around Makkovik is volumetrically
48 and spatially limited compared to the contemporaneous magmatism on the conjugate
49 southwest Greenland margin. This asymmetry in the spatial extent of the exposed onshore
50 magmatism is consistent with other observations of asymmetry between the conjugate
51 margins of the Labrador Sea, including the total sediment thickness in offshore basins, the
52 crustal structure, and the bathymetric profile of the shelf width. We propose that the
53 magmatic and structural asymmetry observed between these two conjugate margins is
54 consistent with an early rifting phase dominated by simple shear rather than pure shear
55 deformation. In such a setting Labrador would be the lower plate margin to the southwest
56 Greenland upper plate.

57 **INTRODUCTION**

58 Stretching of the continental lithosphere results in rifting and may lead to continental
59 breakup accompanied by seafloor spreading (Eldholm and Sundvor, 1979). The production of
60 pairs of conjugate continental passive margins is the inevitable result of the continental
61 breakup process (Geoffroy, 2005). Although conjugate margins may inherit similar
62 geological and structural components, many aspects of these conjugate pairs often display
63 significant asymmetry.

64 The degree of symmetry displayed between conjugate passive margins has
65 traditionally been linked to the mode by which the preceding rifting occurred (Lister et al.,
66 1986), with models of continental rifting being described as either pure shear (McKenzie,
67 1978), simple shear (Wernicke, 1985), or combinations of these (Lister et al., 1986). Rifting

68 under a pure shear–dominated regime occurs by symmetrical, brittle extension of an upper
69 layer and ductile stretching of a lower layer. The simple shear model of rifting predicts that
70 extension occurs along lithosphere-scale normal faults and/or ductile shear zones usually
71 resulting in an asymmetric rift in cross section (e.g., Lister et al., 1986; Etheridge et al.,
72 1989). The large detachment faults required by simple shear models are claimed to be
73 mechanically problematic (Ranero and Pérez-Gussinyé, 2010); it has also been claimed that
74 both conjugate margins often display characteristics of being the upper plate to the
75 detachment fault (Lavie and Manatschal, 2006). It has also been argued that it is difficult to
76 generate melt under simple shear rifting (Latin and White, 1990). Despite these problems, the
77 simple shear model or derivatives of it are often used to explain various aspects of asymmetry
78 on conjugate margin systems, for example, the South Atlantic margins (Becker et al., 2016).
79 Testable predictions of the detachment model of passive margin formation (Lister et al.,
80 1986) include a wide continental shelf, and deep sag basins overlying the sedimentary synrift
81 fill on the lower plate margin. In contrast, the upper plate margin remains relatively unfaulted
82 with an induced continental drainage divide caused by uplift due to magmatic underplating.

83 In this contribution we assess the degree of asymmetry displayed by the conjugate
84 margins of the Labrador Sea (Fig. 1A) to determine if rifting prior to the formation of these
85 margins is likely to have taken place under a pure or a simple shear–dominated regime. This
86 assessment was achieved through observations made during four weeks of field work
87 between June and July 2015 near the town of Makkovik, Labrador, Canada. The primary aim
88 of the field work was to identify and characterize the spatial extent and field relationships of
89 previously described Mesozoic igneous rocks, which Tappe et al. (2007) related to rifting
90 prior to the opening of the Labrador Sea. Field observations were supplemented by whole-
91 rock geochemistry (X-ray fluorescence, XRF) of igneous rock samples. Our field data are
92 then considered in the context of observations from elsewhere on the margins of the Labrador

93 Sea. We integrate these observations with analysis of large-scale geophysical data sets
94 including that of the National Oceanic and Atmospheric Administration (NOAA; Divins,
95 2003), seismic reflection profiles, and the Smith and Sandwell (1997) global topography data
96 set to further test our interpretation of margin asymmetry.

97 **GEOLOGICAL SETTING**

98 The Labrador Sea separates Labrador in eastern Canada from southwest Greenland
99 (Fig. 1A) and is floored by a small (~900 km wide) oceanic basin that provides an ideal place
100 to study conjugate passive margin pairs where the production of oceanic crust was relatively
101 limited (Chalmers and Laursen, 1995). Rifting of the Labrador Sea has previously been
102 attributed to either a pure shear-type model, based on seismic and other geophysical data
103 indicating that faulting is confined to the upper crust (Keen et al., 1994), or a simple shear-
104 type model, based on observations of the asymmetry of the transition zones (Chian et al.,
105 1995a).

106 Rifting prior to the opening of the Labrador Sea started as early as the Late Triassic to
107 Jurassic, based on ages obtained from dike swarms in West Greenland that are interpreted to
108 be related to early rifting (Larsen et al., 2009) (Fig. 1A). The early seafloor spreading history
109 of the Labrador Sea is poorly constrained, with the oldest undisputed magnetic anomaly
110 interpretation in the Labrador Sea being from polarity chron 27 (C27; Danian; Chalmers and
111 Laursen, 1995). However, seafloor spreading may have initiated earlier, at C32 (Campanian)
112 in the southern Labrador Sea and C28 (Maastrichtian) in the northern Labrador Sea
113 (Srivastava, 1978). Seafloor spreading in the Labrador Sea underwent a major reorganization
114 and change in spreading direction at C24–C25N (Thanetian–Ypresian) (Fig. 1B), coincident
115 with the onset of North Atlantic spreading (Srivastava, 1978). After the reorganization of the
116 North Atlantic and Labrador Sea between C24 and C25N there was a reduction in the rate of

117 seafloor spreading before it eventually ceased at C13N (Eocene-Oligocene boundary)
118 (Geoffroy, 2001).

119 The sedimentary basins offshore Labrador record the progressive opening of the
120 Labrador Sea from south to north (DeSilva, 1999) during the Mesozoic. Two major
121 sedimentary basins are present off the coast of Labrador (DeSilva, 1999): the Hopedale Basin
122 in the south and the Saglek Basin to the north (Fig. 1A). Both the Saglek and Hopedale
123 Basins contain synrift and postrift, clastic-dominated sequences of Cretaceous to Pleistocene
124 age (Jauer et al., 2014). Exposures of Mesozoic and Cenozoic sediments onshore along the
125 Labrador coast are extremely rare (Haggart, 2014).

126 From north to south the basement tectonic units exposed at surface on the coast of
127 Labrador are the Archean Nain Province, the Paleoproterozoic Makkovik Province, and the
128 Mesoproterozoic Grenville Province (LaFlamme et al., 2013; Fig. 2). The Makkovik
129 Province is separated from the Nain Province by the Kanairiktok shear zone (Culshaw et al.,
130 2000) and from the Grenville Province by the Grenville Front, which marks the northern limit
131 of widespread Grenvillian deformation (Funck et al., 2001). The Makkovik Province is
132 characterized as a Paleoproterozoic accretionary belt and is the smallest defined tectonic
133 component of the Canadian shield (Ketchum et al., 2002). Prior to the opening of the
134 Labrador Sea the Makkovik Province was adjacent to the Ketilidian mobile belt (KMB; Fig.
135 2), which currently forms part of southwest Greenland (e.g., Garde et al., 2002; Wardle et al.,
136 2002; Kerr et al., 1997). The Makkovik Province can be separated into three distinct zones
137 with distinctive geological characteristics (Kerr et al., 1996); from northwest to southeast,
138 they are the Kaipokok, Aillik, and Cape Harrison domains (Fig. 2) (Kerr et al., 1997).

139 **Onshore Rift-Related Magmatism on the Margins of the Labrador Sea**

140 Our field work was carried out in the Aillik domain of the Makkovik Province. Here,
141 the Early Cretaceous nephelinite suite (ca. 142 Ma) located near Makkovik (Fig. 3; Table 1)

142 is the most recent of three magmatic events identified by Tappe et al. (2007). The older two
143 magmatic events formed a Neoproterozoic ultramafic lamprophyre and carbonatite dike suite
144 (ca. 590–555 Ma) and a Mesoproterozoic olivine lamproite dike suite (ca. 1374 Ma) (Tappe
145 et al., 2006). These two older events are not considered to be directly related to the rifting that
146 culminated in the Mesozoic opening of the Labrador Sea (Tappe et al., 2007).

147 The Tappe et al. (2007) nephelinite suite (Fig. 3; Table 1) comprises fine-grained
148 olivine melilitite, nephelinite, and basanite dikes and sills as much as 2 m thick with a
149 preferential east-west orientation, and has been characterized as a type of rift-related
150 magmatism. This intrusive suite was claimed by Tappe et al. (2007) to be analogous to the
151 coast-parallel alkaline basaltic dikes observed between 60° and 63°N in West Greenland
152 (Larsen, 2006). The samples categorized by Tappe et al. (2007) as belonging to the
153 nephelinite suite are summarized in Table 1, along with their relationship to the samples
154 collected and our analyses (described herein). Here we use the definition of Le Bas (1989) of
155 a nephelinite as containing >20% normative nepheline.

156 Magmatism in West Greenland has also been attributed to early rifting, prior to the
157 opening of the Labrador Sea. According to Larsen et al. (2009) this magmatism is manifest as
158 Mesozoic–Paleogene intrusive rocks that range in scale and abundance from large, coast-
159 parallel dike swarms to small, poorly exposed dike swarms or single intrusions (Fig. 1; Table
160 2). The large coast-parallel dikes extend for 380 km along the southwest Greenland coast
161 (Larsen et al., 1999). Chalmers et al. (1995) described the later Paleogene breakup-related
162 flood basalts farther north in and around the Davis Strait, but these are beyond the
163 geographical and temporal scope of this study. The igneous rocks observed onshore
164 southwest Greenland (Table 2) demonstrate that multiple magmatic events occurred on this
165 margin during and after the Mesozoic. Although many of these events are likely to be rift

166 related, it is extremely unlikely that all these igneous rocks were produced due to the same
167 event.

168 **Offshore Rift-Related Magmatism on the Margins of the Labrador Sea**

169 Mesozoic magmatism has also been observed and documented in exploration wells on
170 the Labrador shelf (Fig. 1A; Table 3) (Umpleby, 1979). Volcanic rocks that are believed to
171 have been erupted during the early stages of rifting are mostly assigned to the Alexis
172 Formation; the type section is recorded in the Bjarni H-81 well (e.g., Ainsworth et al., 2014;
173 Umpleby, 1979). Here a sequence of basalts interspersed with sandstones and silty clays was
174 recorded, but no pyroclastic rocks were documented (Umpleby, 1979). Two cores from the
175 Alexis Formation in Bjarni H-81 have been dated using K-Ar bulk-rock analysis. The
176 lowermost core came from 2510 m and basaltic rocks have been dated as 139 ± 7 Ma
177 (Valanginian), while those in the upper core at 2260 m were dated as 122 ± 6 Ma (Aptian).
178 The age of the lower core is deemed to be less reliable due to alteration; Umpleby (1979)
179 suggested that the inferred duration of ~17 m.y. for the magmatic event resulting in the
180 eruption of the Alexis Formation is too long and that the lower core might be younger.

181 The total thickness and areal extent of the basalts of the Alexis Formation is not well
182 constrained, beyond the occurrence of volcanic rocks in the Leif M-48, Robertval K-92,
183 Bjarni H-81, Indian Harbour M-52, and Herjolf M-92 wells (Fig. 1A). The Alexis Formation
184 occurs in the Hopedale Basin (Hamilton and Harrison subbasins) and within the southern part
185 of the Saglek Basin, but has not been recorded in the more northern Nain subbasin within the
186 Hopedale Basin (Ainsworth et al., 2014). The thickest recorded occurrence of the Alexis
187 Formation is 357 m in the Robertval K-92 well (Ainsworth et al., 2014). Note that some
188 igneous rocks intersected by wells on the Labrador Shelf have not been assigned to a
189 formation (Ainsworth et al., 2014). Occurrences of unclassified igneous rocks include the
190 “Tuff” and “Diabase” intervals (Canada-Newfoundland and Labrador Offshore Petroleum

191 Board, 2007) in Rut H-11 and the sediments derived from volcanic material in Snorri J-90
192 (McWhae et al., 1980).

193 Although no exploration wells have been drilled on the continental shelf offshore
194 southwest Greenland, Site 646 (Leg 105 of the Ocean Drilling Program, ODP) was drilled on
195 oceanic crust in the southern Labrador Sea (Fig. 1A). With the exception of the oceanic crust,
196 Site 646 did not encounter igneous rocks; however, sediments containing clasts of mafic
197 material were described (Shipboard Scientific Party, 1987).

198 **FIELD OBSERVATIONS OF MESOZOIC MAGMATISM NEAR MAKKOVIK,** 199 **LABRADOR**

200 The aim of the field work was to characterize the nature and extent of Mesozoic
201 magmatism near Makkovik to gain insights into rifting in the region prior to the opening of
202 the Labrador Sea. Our field study of the Mesozoic magmatism near Makkovik was guided by
203 the description of the Early Cretaceous magmatism in Tappe et al. (2007) (Fig. 3; Table 1).
204 Of the nine locations where Tappe et al. (2007) documented Early Cretaceous magmatism,
205 we visited seven sample locations (with exception of L59 and ST217). Eight samples of
206 igneous material were obtained at four of the seven locations visited during this study. Where
207 appropriate, samples collected adjacent to the dikes are also described to provide geological
208 context and to emphasize the field relationships observed for the dikes.

209 At three of the Tappe et al. (2007) sample locations (ST100, ST102, and ST245; Fig.
210 3) we were unable to locate the in situ dikes reported by them. Descriptions including
211 mineralogy, texture, and orientation of all the samples are available in the supplemental data
212 (Supplemental Materials 1¹). Details of the locations, coordinate systems, and the relationship
213 between samples in this work and Tappe et al. (2007) are also available in the supplemental
214 data (Supplemental Materials 2²).

215 **Sample Locations, Field Relationships, and Structural Analysis**

216 ***Makkovik Peninsula***

217 The three samples with the prefix AP1 represent the three dikes found on the
218 peninsula north of the town of Makkovik (Fig. 3), locally referred to as the Hill. The outcrops
219 from which these samples were obtained are on the southern end of a beach (Fig. 4) that
220 marks the intersection between a large linear gully that extends 1 km inland on a bearing of
221 198°, and the western coast of the peninsula. The dikes that provided samples AP1-S1 and
222 AP1-S2 are well exposed, but the dike from which AP1-S3 was collected is only fully
223 exposed during low tide.

224 AP1-S1 and AP1-S2 were collected from two different parallel dikes in an
225 approximately north-south orientation (Fig. 4), and are ~1 m and ~2 m thick, respectively.
226 The dike that provided sample AP1-S3 is oriented approximately east-west and is much
227 smaller than the north-south dikes, being only ~30 cm wide. The dike from which AP1-S3
228 was obtained is crosscut by the dike from which AP1-S2 was obtained. The age relationship
229 between AP1-S1 and AP1-S2 could not be determined from field relationships.

230 ***Ford's Bight***

231 Ford's Bight is the elongate bay between Ford's Bight Point and Cape Strawberry,
232 where three of the nine occurrences of Early Cretaceous magmatism reported by Tappe et al.
233 (2007) are located (Fig. 3). Samples in this study with the prefix AP2 were collected at the
234 Tappe et al. (2007) location ST103 on the eastern side of Ford's Bight (Figs. 3 and 5A), with
235 the exception of AP2-S6, which was collected 45 m away from AP2 on a bearing of 025°
236 (Fig. 5B). At the location of AP2 (Fig. 5B), a poorly exposed outcrop within the intertidal
237 range (Figs. 5C, 5D) contained two dikes (sites of samples AP2-S1 and AP2-S2), within a
238 diatreme breccia (samples AP2-S5 and AP2-S6) in proximity to exposed metamorphosed
239 basement (samples AP2-S3 and AP2-S4) (Fig. 5C). An overview of the spatial relationship
240 between the lithologies at AP2 is provided in Figures 5B and 5C. Although we visited sites

241 ST100, ST102, and ST103 (Fig. 5A) during our field study, no in situ outcrop was found at
242 ST100 and ST102; however, small boulders, as wide as 1 m, of the breccia material similar to
243 that observed in samples AP2-S5 and AP2-S6 were observed at these locations.

244 The dike from which sample AP2-S1 (Fig. 5) was collected (dike 1) is oriented
245 approximately north-south, whereas the dike from which sample AP2-S2 was obtained (dike
246 2) is oriented approximately east-west. Both dikes vary in thickness along their observable
247 length; dike 1 varies in thickness from 25 to 40 cm and dike 2 varies from 20 to 30 cm. At the
248 AP2 location it was observed that dike 2 crosscuts dike 1, and thus the east-west-oriented
249 dike 2 is younger.

250 *Cape Strawberry*

251 Cape Strawberry is a large headland between Ford's Bight and Big Bight to the
252 northeast of Makkovik. Tappe et al. (2007) described Early Cretaceous magmatism on Cape
253 Strawberry at two locations (ST254 and ST253; Fig. 3). We collected sample AP3-S1 in
254 proximity to ST253 (Fig. 6). ST254 is the location of the only sample in the Early Cretaceous
255 suite that was been dated by $^{40}\text{Ar}/^{39}\text{Ar}$ methods (141.6 ± 1.0 Ma) by Tappe et al. (2007), and
256 it is also the only location situated inland (Fig. 3). While it is an area of relatively good
257 exposure (Fig. 7) of the 1720 Ma Cape Strawberry Granite (Hinchey, 2013), no nephelinite
258 dikes were observed at this location or anywhere in the vicinity. Thus we were unable to
259 establish field relationships or acquire an equivalent sample for further analysis.

260 *North of Ikey's Point*

261 Ikey's Point is located on the southeastern side of the large peninsula north of
262 Makkovik (Fig. 3). Two dike samples were collected from the area north of Ikey's Point, at
263 the site of previously reported Mesozoic magmatism, and are denoted with the prefix AP4
264 (Fig. 8). Sample AP4-S1 was collected ~15 m south of ST245, and sample AP4-S2 was
265 collected on a separate dike a further 5 m south of AP4-S1.

266 Samples AP4-S1 and AP4-S2 are both oriented approximately east-west and display
267 multiple bridge structures (Fig. 8C). The dikes are <13 cm and 25 cm thick for AP4-S1 and
268 AP4-S2, respectively. No crosscutting relationships were observed between AP4-S1 and
269 AP4-S2, thus relative ages could not be determined for the AP4 dikes.

270 **Structural Analysis**

271 An overview of the orientations of the dikes sampled during this study is provided in
272 Figure 9. AP3-S1 is not included in Figure 9 because this sample was obtained from a
273 boulder (Fig. 6B). Figure 9A demonstrates that the dikes sampled by this study do not appear
274 to be part of a singular, systematic dike swarm. Figure 9B demonstrates that none of the dikes
275 analyzed during our study at locations where Mesozoic magmatism has been documented
276 previously are margin parallel, i.e., striking 130°–150°. Margin-parallel orientations might be
277 the predominant trend expected for dikes intruded during rifting, unless a stress reorientation
278 occurred at the rift margin (e.g., Philippon et al., 2015).

279 **Lithological Descriptions and XRF Analysis**

280 In the following section lithologies are described and the results of XRF analysis
281 (Supplemental Materials 3³) on the samples obtained by this study are presented. Thin
282 sections in both plane and cross-polarized light are presented in Figure 10; full descriptions to
283 complement those given in this section are provided in the Supplemental Materials 1 (see
284 footnote 1).

285 ***Makkovik Peninsula***

286 The gray dike from which sample AP1-S1 was obtained has an extremely fine-grained
287 groundmass that surrounds a main phenocryst phase of clinopyroxene (60%), which is
288 generally arranged into star-shaped clusters of two or more crystals. Highly altered olivine
289 (15%) is also present, along with apatite (<5%), amphibole (<5%), and biotite (<5%). Some
290 vesicles infilled with calcite were as much as 6 mm wide, but most were ~2 mm wide. There

291 is no observable metamorphic mineral fabric in AP1-S1. The SiO₂ content of sample AP1-S1
292 is too low to use the total alkalis versus silica (TAS) classification (Le Bas et al., 1986), but
293 it can be classified as a lamprophyre (Woolley et al., 1996; Rock, 1986) due to the mineral
294 assemblage and composition. Lamprophyre dikes are well studied and known to be extensive
295 in the area (Foley, 1989).

296 Sample AP1-S2 was collected from a dark green dike. The most abundant mineral
297 phase is chlorite (50%), which occurs as clusters of multiple crystals in the groundmass. This
298 sample also contains altered plagioclase (30%), amphibole (10%), and apatite (<2%). No
299 metamorphic mineral fabric was observed in sample AP1-S2. Sample AP1-S2 was classified
300 as a basanite according to the TAS classification (Le Bas et al., 1986).

301 The dike from which sample AP1-S3 was obtained has a red-brown weathered surface
302 and a blue-gray clean surface. The most abundant mineral phase in AP1-S3 is plagioclase
303 (60%) occurring as highly altered interlocking crystals. Chlorite (25%) is the next most
304 abundant mineral phase and occurs as both individual crystals and clusters. Other minerals
305 present with abundances <5% in sample AP1-S3 include: amphibole, titanite, apatite, and
306 pyrite. As with the other two samples collected at AP1, no mineral fabric is present in AP1-
307 S3. Sample AP1-S3 was classified as a basaltic trachyandesite according to the TAS
308 classification (Le Bas et al., 1986).

309 In addition to the different mineral assemblages, all the samples analyzed from the
310 AP1 location have notably different compositions according to the XRF data (Table 4) with
311 the alkali (Na₂O + K₂O) content of the AP1 samples not being as variable as the SiO₂ content
312 (Fig. 11). The XRF data from the Makkovik Peninsula shows that SiO₂ content is lowest in
313 AP1-S1 and highest in AP1-S3, which is the most felsic of all the samples analyzed. The
314 sample with the composition most similar to the data collected by Tappe et al. (2007) is AP1-
315 S1. In summary, the AP1 samples (AP1-S1, AP1-S2 and AP1-S3) have been classified as

316 olivine lamprophyre, basanite, and basaltic trachyandesite, respectively. Of particular note
317 however, was the absence of the mineral phase nepheline in all the samples collected at this
318 location.

319 ***Ford's Bight***

320 Samples AP2-S1 and AP2-S2 were obtained from two separate dikes but are virtually
321 indistinguishable from one another in thin section (Fig. 10), both texturally and
322 mineralogically. The main mineral phases in both AP2-S1 and AP2-S2 are melilitite (70%)
323 and olivine (20%), resulting in our classification of these dikes as olivine melilitite according
324 to the classification of Woolley et al. (1996). Olivine melilitite is the expected composition at
325 this location according to previous work by Tappe et al. (2007). No metamorphic mineral
326 fabric was observed in either AP2-S1 or AP2-S2.

327 The XRF major element analysis of AP2-S1 and AP2-S2 demonstrates that these
328 samples have very similar compositions (Fig. 11; Table 4). There are, however, several small,
329 but notable compositional differences between these two dikes in that sample AP2-S1 has
330 slightly higher SiO₂ and total alkali values than sample AP2-S2 (Fig. 11). Comparison of the
331 major element XRF data obtained from our AP2 dike samples (AP2-S1 and AP2-S2) with the
332 major element composition of sample ST103 (Fig. 11) obtained by Tappe et al. (2007)
333 demonstrates that all three of these samples have very similar compositions and may
334 represent samples collected from the same dike.

335 The two types of metamorphosed basement observed at the AP2 sample sites are an
336 amphibolite (sample AP2-S3) and quartzite (sample AP2-S4) (Figs. 5B, 5C). Sample AP2-S3
337 contains amphibole (45%), highly altered plagioclase (35%), epidote (10%), and chlorite
338 (10%). Sample AP2-S4 contains quartz (80%), garnet (7%), calcite (7%), plagioclase (4%),
339 and opaque minerals (2%). Both samples AP2-S3 and AP2-S4 display a distinct metamorphic
340 mineral fabric (Supplemental Materials 1; see footnote 1). The exposure of these lithologies

341 is limited to a few square meters. However, both dikes (samples AP2-S1 and AP2-S2) were
342 observed to continue into these metamorphosed units (Figs. 5B, 5C). The extent of the
343 continuation of the younger dikes into the metamorphic basement could not be quantified due
344 to lack of exposure.

345 The final lithology present at the AP2 sample site is a diatreme breccia that hosts the
346 two dikes (samples AP2-S1 and AP2-S2). The diatreme breccia was observed as two distinct
347 varieties, as characterized in samples AP2-S5 and AP2-S6. Sample AP2-S5 was taken from
348 the breccia located at AP2 (Figs. 5C, 5D) but is also representative of the nearby boulders on
349 the beach (Figs. 5A, 5E), whereas sample AP2-S6 was taken from a large boulder 45 m away
350 from the rest of the AP2 samples on a bearing of 025° (Fig. 5E). AP2-S5 is green in outcrop,
351 whereas AP2-S6 is dark yellow. This color variation is a reflection of AP2-S5 having a
352 higher ratio of clasts to matrix compared to AP2-S6. The clast types found in both the breccia
353 samples are very similar, mostly consisting of highly variable amounts of quartzite basement,
354 amphibolite dike, olivine melilitite dike, and fragments of individual crystals primarily
355 including but not limited to quartz, olivine, microcline feldspar, and plagioclase. Most clasts
356 are angular, except the melilitite inclusions, which are typically rounded with an undulose
357 texture at their perimeters. Clast size in both AP2-S5 and AP2-S6 is extremely variable,
358 ranging from <0.1 mm to >10 cm. The matrix in both the AP2-S5 and AP2-S6 samples is
359 predominantly carbonate.

360 *Cape Strawberry*

361 The eastern tip of Cape Strawberry (AP3, Fig. 3) is an area of exceptionally well
362 exposed basement rocks (Fig. 6A) that were not observed to be intruded by dikes of any type.
363 However, a distinct gully (Fig. 6B) filled with two types of boulders (granite and a mafic
364 igneous material) was noted. The mafic igneous material in this gully provided sample AP3-
365 S1. The boulder from which AP3-S1 was obtained has a red-brown weathered surface and a

366 dark gray clean surface. In hand specimen, calcite-infilled vesicles (to 7 mm) and olivine
367 phenocrysts are visible. The dominant mineral phases in this sample are olivine, both fresh
368 (20%) and serpentinized (15%), along with clinopyroxene in the groundmass (25%) and as a
369 larger crystal phase (15%). The SiO₂ content of sample AP1-S1 is too low to use the TAS
370 classification (Le Bas et al., 1986), but it can be classified as a lamprophyre (Woolley et al.,
371 1996; Rock, 1986) due to the mineral assemblage and composition.

372 The XRF major element analysis of AP3-S1 (Fig. 11; Table 4) demonstrates that it is
373 compositionally very similar to the igneous rocks sampled by Tappe et al. (2007) near this
374 location, having a nearly identical SiO₂ value but slightly lower alkali content. However,
375 given that AP3-S1 does not contain the mineral phase nepheline, as expected the dike from
376 which AP3-S1 was collected does not belong to the nephelinite suite. The nearest in situ
377 outcrop of the olivine lamprophyre composing the boulders in the gully was 120 m away
378 from the location of ST253 (Fig. 6C).

379 *North of Ikey's Point*

380 In outcrop the weathered surface of the dike from which sample AP4-S1 was obtained
381 varies from dark gray through to reddish-brown. The dominant mineral phase in sample AP4-
382 S1 is clinopyroxene, occurring in both the groundmass (40%) and as larger crystals (20%).
383 Olivine also occurs in AP4-S1 as a serpentinized (10%) and unaltered variety (5%). Vesicles
384 with a calcite infill are common in AP4-S1. The XRF data obtained from AP4-S1 (Fig. 11;
385 Table 4) indicate that this sample is a basanite according to the TAS classification of Le Bas
386 et al. (1986).

387 Sample AP4-S2 was obtained from a separate dike 5 m south of the dike from which
388 sample AP4-S1 was collected (Fig. 8). This second dike is slightly wider, 25 cm; in outcrop it
389 is brown and more fractured and weathered than the previous dike. Sample AP4-S2 contains
390 clinopyroxene (50%), plagioclase (20%), and olivine. Some minor opaque minerals are also

391 present in AP4-S2 along with numerous calcite-infilled vesicles. AP4-S2 was classified as a
392 basanite based on the major element composition derived using XRF and plotted on a TAS
393 diagram (Fig. 11).

394 Although both AP4-S1 and AP4-S2 were classified as basanites, slight compositional
395 differences between the two samples are apparent in the XRF major element data (Fig. 11;
396 Table 4). These results show that AP4-S2 has a slightly higher SiO₂ and alkali content than
397 AP4-S1. Given this slight compositional variation between these two dikes, it is very likely
398 that these two dikes represent the same magmatic event, particularly given the similar
399 orientations (Fig. 9). Overall our observations and analysis of the data collected at the AP4
400 location in the area north of Ikey's Point indicate that Early Cretaceous magmatism north of
401 Ikey's Point may comprise two small (13 and 25 cm wide) basanite dikes.

402 **BATHYMETRY, SEDIMENT THICKNESS, AND CRUSTAL STRUCTURE**

403 An analysis of the degree of symmetry displayed in the bathymetry, sediment
404 thickness, and crustal structure of the conjugate margins of the Labrador Sea is presented
405 here to complement the asymmetry shown in the magmatic distribution in the preceding
406 discussion (Fig. 12). To assess the margin symmetry displayed in the NOAA total sediment
407 thickness (Whittaker et al., 2013) data and the global bathymetry data set (Smith and
408 Sandwell, 1997), profiles approximating the traces of seismic lines BGR77-17, BGR77-21,
409 and BGR77-12 (Fig. 1A) were created (Fig. 12). These profiles were then extended along the
410 same trajectory as their corresponding seismic line until they reached the modern coastline,
411 thus allowing us to study the full width of the continental shelf. Our observations of
412 conjugate margin asymmetry are summarized in Table 5.

413 Figure 12A displays the Smith and Sandwell (1997) global bathymetry data set for the
414 Labrador Sea. The Labrador Sea has a maximum depth of ~3500 m, with water depths mostly
415 <200 m on both continental shelves (Fig. 12B). The continental shelf is ~150 km wide

416 offshore Labrador compared to southwest Greenland, where it is mostly <50 km wide. The
417 profiles (Fig. 12B) show that the continental shelf remains relatively consistent in width
418 along the southwest Greenland margin, whereas on the Labrador margin it increases to the
419 north.

420 The distribution of sediments between the margins of the Labrador Sea is highly
421 asymmetric (Welford and Hall, 2013). The Labrador margin displays considerably thicker
422 and more extensive synrift and postrift sedimentary sequences compared to the southwest
423 Greenland margin (Figs. 12C, 12D, and 13). The Labrador margin is dominated by a large
424 margin-parallel basin containing in excess of ~8000 m of sediments for much of its length
425 (Fig. 12C). This basin is particularly prominent in the central and northern segments of the
426 margin, where isolated areas contain more than ~11,000 m of sediment infill. Even outside
427 this main basin it can be seen that for a large region extending from ~50 km to ~300 km
428 offshore, a more diffuse area containing ~3000–6000 m of sediment infill is present. This
429 region is much wider at the northern end of the margin compared to the south. In contrast,
430 sediment infill on the southwest Greenland margin is significantly thinner and less spatially
431 extensive than its Labrador conjugate. On the southwest Greenland margin sedimentary
432 basins with thicknesses in excess of 4000 m are absent, with most areas containing <2000 m
433 of sedimentary infill. Thus, comparison of sediment thickness along profiles 1, 2, and 3 (Fig.
434 12D) supports the observation of significantly more sediment deposition on the Labrador
435 margin consistently along the length of the margin. It is interesting that the distance between
436 the start of the profile (modern coastline) and the point of greatest sedimentary thickness
437 appears to decrease from profile 1 in the south to profile 3 in the north. Profiles 1–3 in Figure
438 12D also demonstrate the differing basin geometry between these conjugate margins. On the
439 Labrador margin the main margin-parallel basin appears to represent a distinct feature

440 compared to the southwest Greenland margin where the sedimentary basins, if present,
441 appear to have a less well defined, more diffuse appearance.

442 The crustal velocity model depicted in Chian et al. (1995b) that incorporates the data
443 from Chian and Loudon (1994) was used to assess asymmetry displayed in the crustal
444 structure between the Labrador and southwest Greenland margins (Fig. 14). Previously
445 workers (Keen et al., 1994; Chian and Loudon, 1994; Chian et al., 1995a) considered the
446 velocity structure of both the southwest Greenland and Labrador margins to be divided into
447 three distinct zones (Fig. 14).

448 Zone 1 is characterized as a region that has a typical continental crustal velocity
449 structure. On the Labrador margin zone 1 is ~140 km wide and is characterized by highly
450 extended continental crust that has undergone considerable subsidence. However, on the
451 southwest Greenland margin zone 1 is only ~70 km wide and has undergone considerably
452 less subsidence (Chian, et al., 1995a). Zone 2 represents a region of transitional crust located
453 oceanward of zone 1 on both margins (Chian et al., 1995a). Compared to zone 1, zone 2
454 displays similar velocity characteristics, and is ~70–80 km wide on both margins. Zone 2 is
455 characterized by a 5-km-thick region with a high velocity (6.4–7.7 km/s) overlain by a thin
456 (<2 km) low-velocity region (4–5 km km/s). Zone 3 is characterized by typical oceanic
457 crustal velocities and is oceanward of zone 2 on both margins.

458 **DISCUSSION**

459 **Comparison of the Composition of the Makkovik Magmatism with Other Rift-Related** 460 **Magmatism**

461 The XRF results obtained during this study have been compared to other selected
462 occurrences of rift-related magmatism globally (Fig. 15). The Yarmony Mountain lavas of
463 the Rio Grande Rift (Leat et al., 1990) were selected for comparison because they are
464 interpreted to represent small-volume, early rift-related melts, and therefore may have been

465 produced in a geological setting similar to that of the proposed Early Cretaceous magmatism
466 near Makkovik (Tappe et al., 2007). The Suez Rift magmatism (Shallaly et al., 2013) was
467 selected because it contains a wide array of rift-related manifestations of magmatism,
468 including sills, dikes, and extrusives. Two magmatic suites attributed to the Central Atlantic
469 Magmatic Province (CAMP) are also included for comparison: Algarve in southern Portugal
470 (Martins et al., 2008) along with the magmatism in Guyana and Guinea (Deckart et al., 2005).
471 The CAMP magmatism was selected because it enables comparison with a widespread rift-
472 related magmatic event that resulted in continental breakup.

473 Comparing the composition of the Makkovik Early Cretaceous nephelinite suite
474 (Tappe et al., 2007) with other selected occurrences of rift-related magmatism shows that it is
475 compositionally more diverse than any of the other magmatic suites considered (Fig. 15),
476 displaying greater variation in both the alkali and silica values than any of these systems.
477 Although it is extremely unlikely that all of the AP samples belong to the Early Cretaceous
478 nephelinite suite (particularly sample AP1-S3), the more mafic AP samples depict a similar
479 range of silica values to the Early Cretaceous nephelinite suite. The Tappe et al. (2007)
480 samples show considerably higher variation in total alkali values than the AP samples or any
481 of the other data sets included for comparison. The wide range of compositions found in the
482 Early Cretaceous nephelinite suite (Tappe et al., 2007) may imply that not all of the dikes
483 analyzed by the previous work are part of the same event.

484 **Extent of Mesozoic Magmatism Around Makkovik**

485 Given the relatively close proximity of Makkovik to observations of Early Cretaceous
486 magmatism in offshore wells (Fig. 1; Table 2), it would not be unreasonable to observe
487 evidence of contemporaneous early rift-related magmatism cropping out onshore. Our field
488 observations, however, indicate that the Early Cretaceous magmatism around Makkovik is
489 volumetrically and spatially extremely minor compared to the numerous stages of extensive,

490 readily observable intrusive magmatism that preceded it (e.g., Foley, 1989) and the well-
491 documented magmatism on the conjugate southwest Greenland margin (Larsen et al., 2009).
492 Although the field study area around Makkovik (Fig. 3) is significantly smaller than the
493 extent of the dikes observed in southwest Greenland, no other evidence for Mesozoic
494 magmatism has been recorded elsewhere onshore Labrador.

495 Of the seven sample locations in Tappe et al. (2007) visited during this study none
496 provided clear, undisputable evidence for belonging to a contiguous Early Cretaceous
497 magmatic event. We think it is also exceptionally unlikely that the outcrops were removed by
498 subsequent erosion between this study and the work of Tappe et al. (2007). Our observations
499 on the peninsula north of the town of Makkovik (AP1) and on Cape Strawberry (AP3) did not
500 provide sufficient evidence for the Early Cretaceous magmatism previously described at
501 these locations. The most reliable evidence confirmed by this study for the magmatism
502 characterized by Tappe et al. (2007) as Early Cretaceous was found in Ford's Bight (AP2,
503 Fig. 5) and north of Ikey's Point (AP4, Fig. 8).

504 Our AP2 sample location in Ford's Bight is in very close proximity to the diatreme
505 originally described as a sedimentary breccia by King and McMillan (1975) and later as a
506 diatreme by Wilton et al. (2002). Our field observations concur with that of Wilton et al.
507 (2002) that the AP2 sample location is part of the previously documented Ford's Bight
508 diatreme. This confirms that of the nine samples stated as belonging to the Mesozoic dike
509 suite in Tappe et al. (2007) (Table 1), three are part of a diatreme, not a dike swarm as
510 previously claimed, with two of the Ford's Bight samples locations not containing in situ
511 outcrop. Within the diatreme there are dikes present, but it is misleading to imply that they
512 are part of a singular geographically widespread intrusive event that can be described as the
513 nephelinite suite. The diatreme was mentioned in Tappe et al. (2007, p. 438) as "poorly
514 described mafic dikes cutting a breccia bed"; however, it is not made clear that this area is

515 either (1) the location of three of their samples or (2) a diatreme rather than a dike swarm.
516 Furthermore, confirming that ST103 is, as expected, an olivine melilitite demonstrates that
517 there is unlikely to be a problem associated with the original acquisition or our use of the
518 coordinates provided by Tappe et al. (2007) and the original characterization of the
519 mineralogy at ST103. The geological context of the dikes needs clarifying, because the
520 observed dikes in Ford's Bight are intrinsically associated with the diatreme (Wilton et al.,
521 2002) and do not appear to be associated with a regional-scale intrusive event such as that
522 described in Tappe et al. (2007). However, if the biostratigraphic age provided by King and
523 McMillan (1975) of 197–145 Ma is correct, then this is currently the most reliable evidence
524 in the area for Mesozoic magmatism, with the fossils possibly being derived from the maar
525 above the diatreme (White and Ross, 2011).

526 Our analysis also indicates that one of the dikes north of Ikey's Point at AP4 is likely
527 to be that described and sampled by Tappe et al. (2007), the other basanite dike at this
528 location being part of the same event. However, even if one or both of the dikes at AP4 is the
529 dike analyzed by Tappe et al. (2007), they are extremely small (13 cm and 25 cm wide) and
530 localized.

531 Comparison of the XRF data with other suites of rift-related magmatism globally has
532 demonstrated that the nephelinite suite (Tappe et al., 2007) is compositionally much more
533 diverse than the other events considered (Fig. 15). This observation provides further evidence
534 that the samples collected by Tappe et al. (2007) might not form part of the same magmatic
535 event.

536 Overall, our comparison of the field relationships, orientation, mineralogy, and
537 composition of the samples collected at the locations of the samples prefixed with AP2 and
538 AP4, where some evidence for the Early Cretaceous magmatism described by Tappe et al.

539 (2007) was found, suggests that there is no reason to attribute the exceptionally different style
540 of magmatism at in Ford's Bight (AP2) and north of Ikey's Point (AP4) to the same event.

541 Furthermore, given that the one location in this dike suite that was dated by $^{40}\text{Ar}/^{39}\text{Ar}$
542 methods by Tappe et al. (2007) (sample ST254) was found to not contain any exposed
543 comparable dikes, the coherence of the proposed Early Cretaceous nephelinite suite as being
544 as a result of a singular magmatic event should be reconsidered. In terms of the age of the
545 nephelinite suite characterized by Tappe et al. (2007), the plateau age from the $^{40}\text{Ar}/^{39}\text{Ar}$
546 dating is not defined by a continuous outgassing plateau and the two segments used in each
547 are considerably less than the 50% gas release generally accepted as the hallmark of a reliable
548 step-heating age. Even when the two segments in Tappe et al. (2007) are combined, it seems
549 that the total gas fraction plateau used is only 52%, i.e., only just above 50%. In addition, the
550 problem with the $^{40}\text{Ar}/^{39}\text{Ar}$ date of Tappe et al. (2007) is the fact that the inverse isochron age
551 is well outside of error and the plateau age is far from the atmospheric value. Thus the
552 $^{40}\text{Ar}/^{39}\text{Ar}$ age of 142 Ma for sample ST254 is of marginal reliability.

553 Another aspect of the Early Cretaceous magmatism on the Labrador margin that
554 remains unclear is why the orientations of the dikes observed by Tappe et al. (2007) are
555 described as predominantly east-west. If these dikes are rift related, then they would be
556 expected to have been intruded under the influence of the extensional stress field parallel to
557 the rift axis i.e., coast parallel as they are in southwest Greenland (Larsen et al., 2009).
558 Although the only compositionally appropriate east-west dikes observed by this study were at
559 Ikey's Point (AP4), should a larger suite exist with this orientation it would not be compatible
560 with simple northeast-southwest-trending Mesozoic rifting, culminating in the opening of the
561 Labrador Sea (Abdelmalak et al., 2012).

562 **Implications for Early Rifting of the Labrador Sea Region**

563 The results of this study have demonstrated that considerable asymmetry exists in
564 many aspects of the conjugate margins of the Labrador Sea, including the distribution of rift-
565 related magmatic rocks, the bathymetric expression, the sediment distribution, and the crustal
566 structure. These observations of asymmetry may support a simple shear mode of rifting (Fig.
567 16). Here we systematically evaluate our observations of asymmetry against the predictions
568 of the Lister et al. (1986) simple shear model of passive margin formation that has been
569 previously applied to explain the observed asymmetry in many conjugate margin pairs and
570 rift systems including the Greenland-Norway conjugate margins (Torske and Prestvik, 1991)
571 and the south Atlantic (Becker et al., 2016). Of particular importance when evaluating the
572 simple shear model (Lister et al., 1986) is whether the polarity of the different aspects of
573 asymmetry all agree with the predictions of the model.

574 A full comparison of the extent of rift-related magmatism on the margins of the
575 Labrador Sea is inhibited by the absence of well data offshore southwest Greenland (Fig.
576 1A). The nearest offshore well on the Greenland side of the Labrador Sea is Qulleq-1, which
577 is much farther north in the Davis Strait (Fig. 1A), and is influenced more by transform
578 margin tectonics rather than the rifted margin regime in the Labrador Sea (Wilson et al.,
579 2006).

580 Although the absence of well data offshore southwest Greenland prevents us from
581 making a full comparison of the volume of rift-related magmatism, this study has shown that
582 the Early Cretaceous magmatism identified onshore in Labrador by Tappe et al. (2007) is
583 considerably less extensive than that observed on the coast parallel dikes onshore in
584 southwest Greenland (Larsen et al., 2009). This allows us to state that there is an asymmetric
585 distribution in the extent of the exposed onshore Mesozoic magmatism between the Labrador
586 margin and the southwest Greenland margin. This asymmetric distribution of rift-related
587 magmatism supports the predictions of the simple shear model of passive margin formation,

588 whereby the center of the melt generation may have been offset from the central rift axis (Fig.
589 16A), resulting in a greater amount of melt on the upper plate southwest Greenland margin
590 (Fig. 16A). That is, the greater extent of coast-parallel dikes in southwest Greenland suggests
591 that the southwest Greenland margin may represent the upper plate margin in a simple shear
592 system.

593 Magmatic underplating on the upper plate margin is another prediction of the Lister et
594 al. (1986) simple shear model. High-velocity zones have been observed in seismic studies on
595 these conjugate margins, but whether they represent serpentinized peridotite (Reid and Keen,
596 1990) or magmatic underplating (Keen et al., 1994) is debatable (Chian et al., 1995b). Chian
597 et al. (1995b) determined that serpentinized peridotite is more consistent with the
598 observations than magmatic underplating. Due to the inconclusive nature of these
599 observations, we have chosen not to use them as evidence in our analysis of the applicability
600 of the simple shear model (Lister et al., 1986) to the margins of the Labrador Sea. However,
601 magmatic underplating might help to explain the absence of significant postrift sedimentary
602 basins offshore southwest Greenland (Figs. 12C, 12D), as magmatic underplating could
603 provide the additional buoyancy required to prevent significant postrift subsidence from
604 occurring. Alternatively, the lack of postrift sedimentation offshore southwest Greenland
605 could be due to a deficiency of sediment supply to the offshore basins; however, if this was
606 the case we would still expect to observe deeper water depths.

607 Despite the obvious disparity in the extent of onshore rift-related intrusive magmatism
608 between southwest Greenland and that near Makkovik, quantifying the melt volumes
609 associated with rifting on each margin even approximately is problematic for a number of
610 reasons. First, offshore magmatism cannot be accurately quantified on both margins given the
611 sparse seismic and well data coverage. Second, it is difficult to estimate the contributions of
612 magmatic underplating and other intrusives in the lower crust; these contributions were

613 estimated by White (1992) to potentially represent three times the volumes of other intrusive
614 and extrusive magmatic rocks on passive margins. However, it seems more likely that
615 significant magmatic underplating is present in southwest Greenland due to the potential
616 additional support this margin has received.

617 A wider continental shelf on the lower plate margin is another prediction of the simple
618 shear model of passive margin formation (Lister et al., 1986). The asymmetric nature of the
619 bathymetric profiles across the Labrador Sea depicted in this study (Figs. 12A, 12B) using the
620 Smith and Sandwell (1997) bathymetric data is consistent with a model in which the
621 Labrador margin would be the lower plate margin.

622 An asymmetric distribution of sedimentation as described in this study is also a
623 prediction of the simple shear model of passive margin formation (Lister et al., 1986), the
624 greater amount of sedimentary deposition occurring on the lower plate margin. The NOAA
625 total sediment thickness data show that the Labrador margin has considerably deeper
626 sedimentary basins (Figs. 12C, 12D), and thus would represent the lower plate margin in a
627 simple shear system.

628 Another aspect of the sediment distribution on the margins of the Labrador Sea that
629 supports the simple shear model is the geometry of the marginal basins. In the marginal basin
630 on the Labrador margin the total sediment thickness data profile depicts an abrupt increase in
631 sediment thickness, as opposed to the southwest Greenland margin, where a much less
632 apparent peak in sediment thickness is present. This abrupt increase in sediment thickness
633 may imply a fault-controlled basin as opposed to the marginal basins offshore southwest
634 Greenland, in which the NOAA data record more diffuse sedimentation.

635 The simple shear model implies a much greater degree of synrift structuring on the
636 lower plate margin. Our analysis has demonstrated that the Labrador margin displays
637 considerably greater synrift deformation and sedimentation than the southwest Greenland

638 margin. The more significant synrift deformation and sedimentation on the Labrador margin
639 supports a simple shear–dominated mode of early rifting with Labrador being the lower plate
640 margin.

641 Welford and Hall (2013) calculated sediment difference (excess and deficiency), also
642 using the NOAA sediment thickness data for the Labrador Sea. The work of Welford and
643 Hall (2013) showed that most of the Labrador Sea appears from isostatic calculations to be
644 deficient in sediments, whereas the Hopedale Basin is near balanced and the Saglek Basin has
645 an excess of sediments. Welford and Hall (2007) showed that high gradients in the sediment
646 excess and deficiency could indicate the presence of steep listric faults, a key component of a
647 simple shear–dominated rifting regime, supporting a simple shear model of margin formation
648 in the Labrador Sea.

649 The velocity structure of the margins of the Labrador Sea (Fig. 14; Chian et al.,
650 1995b) also displays asymmetry consistent with a simple shear–dominated phase of early
651 rifting. This is evident in zone 1 (stretched continental crust, Fig. 14), where this region is
652 ~140 km wide on the Labrador margin compared to the southwest Greenland margin, where
653 this zone occupies ~70 km. In the simple shear model of passive margin formation the greater
654 amount of stretching, faulting, and subsequent subsidence occurs on the lower plate margin,
655 which, as with the other observations made by this study, would be the Labrador margin.
656 Using their velocity structure, Chian et al. (1995a) proposed a model of continental breakup
657 whereby breakup occurred closer to the southwest Greenland margin. Breakup occurring
658 closer to the southwest Greenland margin is consistent with the other observations implying
659 that southwest Greenland may have constituted the upper plate margin.

660 Overall, the high degree of magmatic, sedimentary, and structural asymmetry
661 observed between these two conjugate margins allows us to suggest a simple shear
662 mechanism of early rifting, as opposed to rifting under a pure shear–dominated regime.

663 Under a simple shear rifting regime the upper plate margin would be southwest Greenland
664 and the lower plate margin would be Labrador, according to the distinction between the
665 margin types in the original model by Lister et al. (1986). The asymmetry documented
666 between these margins may have implications for petroleum exploration in the Labrador Sea
667 (e.g., Jauer et al., 2014; Jauer and Budkewitsch, 2010). Such implications include the deeper,
668 potentially more prospective basins on the Labrador margin and the inevitable asymmetry in
669 the heat flow due to the asymmetric magmatic distribution, which may potentially influence
670 the maturation of source material (Peace et al., 2015).

671 **CONCLUSIONS**

672 This study used the previous descriptions of Mesozoic rift-related magmatism (Tappe
673 et al., 2007) to guide field work with the aim of understanding the controls on rifting in the
674 region prior to the opening of the Labrador Sea. Through the field work and subsequent
675 analysis of the data we have further characterized this event, demonstrating that certain
676 aspects differ from the descriptions provided in the previous work. Our conclusions on the
677 characteristics and extent of Early Cretaceous magmatism in proximity to the town of
678 Makkovik are as follows.

679 1. Early Cretaceous magmatism around Makkovik, Labrador, is volumetrically and
680 spatially extremely minor compared to the numerous other phases of extensive, readily
681 observable intrusive magmatism exposed in the area.

682 2. Of the nine Early Cretaceous magmatism sample locations described by Tappe et
683 al. (2007), we visited seven for this study. Only two of these seven localities provided any
684 evidence for the magmatism described in the previous work.

685 3. Mesozoic magmatism is not sufficiently simple and consistent to consider this
686 event as a single coherent intrusive suite of Early Cretaceous nephelinite dikes, as the
687 outcrops are too sparse, variable, and unreliable. At least three of the Tappe et al. (2007)

688 samples are actually from a diatreme, and the rest are either unobservable or ambiguous in
689 nature.

690 4. The most reliable evidence for Mesozoic magmatism around Makkovik is the
691 diatreme in Ford's Bight dated using fossil evidence by King and McMillan (1975). The
692 diatreme was not observed to be part of a dike swarm as implied by the sample locations in
693 Tappe et al. (2007).

694 Our conclusions on margin asymmetry, rifting mechanisms and the relationship
695 between Mesozoic magmatism in West Greenland and Labrador are the following.

696 1. The magmatic distribution across these two conjugate margins is extremely
697 asymmetric, with the Mesozoic magmatism exposed at surface in the area around Makkovik
698 being minor compared to observations of rift-related diking exposed at surface on the
699 conjugate southwest Greenland margin.

700 2. This asymmetric magmatic distribution complements other observations of
701 asymmetry, including deeper sedimentary basins and a wider continental shelf on the
702 Labrador margin compared to southwest Greenland allowing us to propose a simple shear
703 model for early rifting prior to the opening of the Labrador Sea, as opposed to a pure shear
704 rifting model.

705 3. In a simple shear rifting model the southwest Greenland margin would be the upper
706 plate margin and the Labrador margin would be the lower plate margin.

707 **ACKNOWLEDGMENTS**

708 Funding for this research was primarily provided by Royal Dutch Shell in the form of
709 a CeREES (Centre for Research into Earth Energy Systems) studentship at Durham
710 University. We thank the Durham University Center for Doctoral Training in Energy and the
711 Durham Energy Institute for their contribution toward the costs of this research. This research
712 would not have been possible without the advice of Alana Hinchey of the Geological Survey

713 of Newfoundland and Labrador, and the hospitality of the people of Makkovik. We also
714 thank BGR (Bundesanstalt für Geowissenschaften und Rohstoffe, Hannover, Germany) and
715 Schlumberger Limited for providing access to the seismic data and the Petrel seismic
716 interpretation software, respectively. We acknowledge the contribution of the two anonymous
717 reviewers.

718 **REFERENCES CITED**

- 719 Abdelmalak, M.M., Geoffroy, L., Angelier, J., Bonin, B., Callot, J.P., Gélard, J.P., and
720 Aubourg, C., 2012, Stress fields acting during lithosphere breakup above a melting
721 mantle: A case example in West Greenland: *Tectonophysics*, v. 581, p. 132–143,
722 doi:10.1016/j.tecto.2011.11.020.
- 723 Ainsworth, N.R., Riley, L.A., Bailey, H.W., and Gueinn, J.J., 2014, Cretaceous–Tertiary
724 Stratigraphy of the Labrador Shelf: St. John's, Riley Geoscience Limited for Nalcor
725 Energy, 56 p.
- 726 Becker, K., Tanner, D.C., Franke, D., and Krawczyk, C.M., 2016, Fault-controlled
727 lithospheric detachment of the volcanic southern South Atlantic rift: *Geochemistry,*
728 *Geophysics, Geosystems*, v. 17, p. 887–894, doi:10.1002/2015GC006081.
- 729 Chalmers, J.A., and Laursen, K.H., 1995, Labrador Sea: The extent of continental and
730 oceanic crust and the timing of the onset of seafloor spreading: *Marine and Petroleum*
731 *Geology*, v. 12, p. 205–217, doi:10.1016/0264-8172(95)92840-S.
- 732 Chalmers, J.A., Larsen, L.M., and Pedersen, A.K., 1995, Widespread Palaeocene volcanism
733 around the northern North Atlantic and Labrador Sea: Evidence for a large, hot, early
734 plume head: *Journal of the Geological Society [London]*, v. 152, p. 965–969,
735 doi:10.1144/GSL.JGS.1995.152.01.14.
- 736 Chian, D., and Loudon, K.E., 1994, The continent-ocean crustal transition across the
737 southwest Greenland margin: *Journal of Geophysical Research*, v. 99, p. 9117–9135,

- 738 doi:10.1029/93JB03404.
- 739 Chian, D., Keen, C., Reid, I., and Loudon, K.E., 1995a, Evolution of nonvolcanic rifted
740 margins: New results from the conjugate margins of the Labrador Sea: *Geology*, v. 23,
741 p. 589–592, doi:10.1130/0091-7613(1995)023<0589:EONRMN>2.3.CO;2.
- 742 Chian, D., Loudon, K.E., and Reid, I., 1995b, Crustal structure of the Labrador Sea conjugate
743 margin and implications for the formation of nonvolcanic continental margins: *Journal of*
744 *Geophysical Research*, v. 100, 24239, doi:10.1029/95JB02162.
- 745 Canada-Newfoundland and Labrador Offshore Petroleum Board, 2007, C-NLOPB Wells: St.
746 John's, Newfoundland, Canada-Newfoundland and Labrador Offshore Petroleum Board:
747 Schedule of Wells, <http://www.cnlopb.ca/wells/>.
- 748 Culshaw, N., Brown, T., Reynolds, P.H., and Ketchum, J.W.F., 2000, Kanairiktok shear
749 zone: The boundary between the Paleoproterozoic Makkovik Province and the Archean
750 Nain Province, Labrador, Canada: *Canadian Journal of Earth Sciences*, v. 37, p. 1245–
751 1257, doi:10.1139/e00-035.
- 752 Deckart, K., Bertrand, H., and Liégeois, J.P., 2005, Geochemistry and Sr, Nd, Pb isotopic
753 composition of the Central Atlantic Magmatic Province (CAMP) in Guyana and Guinea:
754 *Lithos*, v. 82, p. 289–314, doi:10.1016/j.lithos.2004.09.023.
- 755 DeSilva, N.R., 1999, Sedimentary basins and petroleum systems offshore Newfoundland and
756 Labrador, *in* Fleet, A.J., and Boldy, S.A.R., eds., *Petroleum Geology of Northwest*
757 *Europe: Proceedings of the 5th Conference on the Petroleum Geology of Northwest*
758 *Europe: Geological Society of London Petroleum Geology Conference Series*, v. 1, p.
759 501–516, doi:10.1144/0050501.
- 760 Divins, D., 2003, *Total Sediment Thickness of the World's Oceans and Marginal Seas:*
761 *Boulder, Colorado, National Oceanic and Atmospheric Administration National*
762 *Geophysical Data Center*, <https://www.ngdc.noaa.gov/mgg/sedthick/sedthick.html>.

- 763 Eldholm, O., and Sundvor, E., 1979, Geological events during the early formation of a
764 passive margin: *Tectonophysics*, v. 59, p. 233–237, doi:10.1016/0040-1951(79)90047-7.
- 765 Etheridge, M.A., Symonds, P.A., and Lister, G.S., 1989, Application of the detachment
766 model to reconstruction of conjugate passive margins, *in* Tankard, A.J., and Balkwill,
767 H.R., eds., *Extensional Tectonics and Stratigraphy of the North Atlantic Margins*:
768 American Association of Petroleum Geologists Memoir 46, p. 23–40,
769 doi:10.1306/M46497C3.
- 770 Foley, S.F., 1989, Emplacement features of lamprophyre and carbonatitic lamprophyre dykes
771 at Aillik Bay, Labrador: *Geological Magazine*, v. 126, p. 29–42,
772 doi:10.1017/S0016756800006129.
- 773 Frei, D., Hutchison, M.T., Gerdes, A., and Heaman, L.M., 2008, Common-lead corrected U-
774 Pb age dating of perovskite by laser ablation – magnetic sectorfield ICP-MS: 9th
775 International Kimberlite Conference Extended Abstract, v. No. 9IKC-A, p. 1–3.
- 776 Funck, T., Loudon, K.E., and Reid, I.D., 2001, Crustal structure of the Grenville Province in
777 southeastern Labrador from refraction seismic data: Evidence for a high-velocity lower
778 crustal wedge: *Canadian Journal of Earth Sciences*, v. 38, p. 1463–1478,
779 doi:10.1139/e01-026.
- 780 Garde, A.A., Hamilton, M.A., Chadwick, B., Grocott, J., and McCaffrey, K.J.W., 2002, The
781 Ketilidian orogen of South Greenland: Geochronology, tectonics, magmatism, and fore-
782 arc accretion during Palaeoproterozoic oblique convergence: *Canadian Journal of Earth*
783 *Sciences*, v. 39, p. 765–793, doi:10.1139/e02-026.
- 784 Geoffroy, L., 2001, The structure of volcanic margins: Some problematics from the North-
785 Atlantic/ Labrador-Baffin system: *Marine and Petroleum Geology*, v. 18, p. 463–469,
786 doi:10.1016/S0264-8172(00)00073-8.
- 787 Geoffroy, L., 2005, Volcanic passive margins: *Comptes Rendus Geoscience*, v. 337, p. 1395–

- 788 1408, doi:10.1016/j.cрте.2005.10.006.
- 789 Haggart, J.W., 2014, New contributions in Baffin Bay/Labrador Sea petroleum exploration
790 and development geoscience: *Bulletin of Canadian Petroleum Geology*, v. 62, p. 213–
791 216, doi:10.2113/gscpgbull.62.4.213.
- 792 Hinchey, A.M., 2013, *Geology of the Makkovik Area, Labrador (NTS 13O/03 and Parts of*
793 *NTS 13O/02): Government of Newfoundland and Labrador, Department of Natural*
794 *Resources Geological Survey Map 2013–07, Open File 013O/0138, scale 1:50000.*
- 795 Holgate, N.E., Jackson, C.A.-L., Hampson, G.J., and Dreyer, T., 2015, Seismic stratigraphic
796 analysis of the Middle Jurassic Krossfjord and Fensfjord formations, Troll oil and gas
797 field, northern North Sea: *Marine and Petroleum Geology*, v. 68, p. 352–380,
798 doi:10.1016/j.marpetgeo.2015.08.036.
- 799 Jauer, C.D., and Budkewitsch, P., 2010, Old marine seismic and new satellite radar data:
800 Petroleum exploration of northwest Labrador Sea, Canada: *Marine and Petroleum*
801 *Geology*, v. 27, p. 1379–1394, doi:10.1016/j.marpetgeo.2010.03.003.
- 802 Jauer, C.D., Oakey, G.N., Williams, G., and Wielens, J.B.W.H., 2014, Saglek Basin in the
803 Labrador Sea, east coast Canada; stratigraphy, structure and petroleum systems: *Bulletin*
804 *of Canadian Petroleum Geology*, v. 62, p. 232–260, doi:10.2113/gscpgbull.62.4.232.
- 805 Keen, C.E., Potter, P., and Srivastava, S.P., 1994, Deep seismic reflection data across the
806 conjugate margins of the Labrador Sea: *Canadian Journal Earth Sciences*, v. 31, p. 192–
807 205, doi:10.1139/e94-016.
- 808 Kerr, A., Ryan, B., Gower, C.F., and Wardle, R.J., 1996, The Makkovik Province: Extension
809 of the Ketilidian mobile belt in mainland North America, *in* Brewer, T.S., ed.,
810 *Precambrian Crustal Evolution in the North Atlantic Region: Geological Society of*
811 *London Special Publication 112*, p. 155–177, doi:10.1144/GSL.SP.1996.112.01.09.
- 812 Kerr, A., Hall, J., Wardle, R.J., Gower, C.F., and Ryan, B., 1997, New reflections on the

- 813 structure and evolution of the Makkovikian-Ketilidian orogen in Labrador and southern
 814 Greenland: *Tectonics*, v. 16, p. 942–965, doi:10.1029/97TC02286.
- 815 Ketchum, J.W., Culshaw, N.G., and Barr, S.M., 2002, Anatomy and orogenic history of a
 816 Paleoproterozoic accretionary belt: The Makkovik Province, Labrador, Canada:
 817 *Canadian Journal of Earth Sciences*, v. 39, p. 711–730, doi:10.1139/e01-099.
- 818 King, A.F., and McMillan, N.J., 1975, A Mid-Mesozoic breccia from the coast of Labrador:
 819 *Canadian Journal of Earth Sciences*, v. 12, p. 44–51, doi:10.1139/e75-005.
- 820 LaFlamme, C., Sylvester, P.J., Hinchey, A.M., and Davis, W.J., 2013, U-Pb age and Hf-
 821 isotope geochemistry of zircon from felsic volcanic rocks of the Paleoproterozoic Aillik
 822 Group, Makkovik Province, Labrador: *Precambrian Research*, v. 224, p. 129–142,
 823 doi:10.1016/j.precamres.2012.09.005.
- 824 Larsen, L.M., 2006, Mesozoic to Palaeogene Dyke Swarms in West Greenland and Their
 825 Significance for the Formation of the Labrador Sea and the Davis Strait: *Geological
 826 Survey of Denmark and Greenland Report*, 69 p.
- 827 Larsen, O., and Møller, J., 1968, K/Ar age determinations from western GreenlandI.
 828 Reconnaissance programme: *Rapport Grønlands Geologiske Undersøgelse*, v. 15, p. 82–
 829 86.
- 830 Larsen, L.M., Rex, D.C., Watt, W.S., and Guise, P.G., 1999, ^{40}Ar - ^{39}Ar dating of alkali
 831 basaltic dykes along the south-west coast of Greenland: Cretaceous and Tertiary igneous
 832 activity along the eastern margin of the Labrador Sea: *Geology of Greenland Survey
 833 Bulletin*, v. 184, p. 19–29.
- 834 Larsen, L.M., Heaman, L.M., Creaser, R.A., Duncan, R.A., Frei, R., and Hutchison, M.,
 835 2009, Tectonomagmatic events during stretching and basin formation in the Labrador
 836 Sea and the Davis Strait: Evidence from age and composition of Mesozoic to Palaeogene
 837 dyke swarms in West Greenland: *Journal of the Geological Society [London]*, v. 166,

- 838 p. 999–1012, doi:10.1144/0016-76492009-038.
- 839 Latin, D., and White, N., 1990, Generating melt during lithospheric extension: Pure shear vs.
840 simple shear: *Geology*, v. 18, p. 327–331, doi:10.1130/0091-
841 7613(1990)018<0327:GMDLEP>2.3.CO;2.
- 842 Lavier, L.L., and Manatschal, G., 2006, A mechanism to thin the continental lithosphere at
843 magma-poor margins: *Nature*, v. 440, p. 324–328, doi:10.1038/nature04608.
- 844 Leat, P.T., Thompson, R.N., Morrison, M.A., Hendry, G.L., and Dickin, A.P., 1990,
845 Geochemistry of mafic lavas in the early Rio Grande Rift, Yarmony Mountain,
846 Colorado, U.S.A: *Chemical Geology*, v. 81, p. 23–43, doi:10.1016/0009-2541(90)90037-
847 8.
- 848 Le Bas, M.J., 1989, Nephelinitic and basanitic rocks: *Journal of Petrology*, v. 30, p. 1299–
849 1312, doi:10.1093/petrology/30.5.1299.
- 850 Le Bas, M.J., Le Maitre, R.W., Streckeisen, A., and Zanettin, B., 1986, A chemical
851 classification of volcanic rocks based on the total alkali silica diagram: *Journal of*
852 *Petrology*, v. 27, p. 745–750, doi:10.1093/petrology/27.3.745.
- 853 Lister, G.S., Etheridge, M.A., and Symonds, P.A., 1986, Detachment faulting and the
854 evolution of passive continental margins: Reply: *Geology*, v. 14, p. 891–892,
855 doi:10.1130/0091-7613(1986)14<891:CARODF>2.0.CO;2.
- 856 Martins, L.T., Madeira, J., Youbi, N., Munhá, J., Mata, J., and Kerrich, R., 2008, Rift-related
857 magmatism of the Central Atlantic magmatic province in Algarve, southern Portugal:
858 *Lithos*, v. 101, p. 102–124, doi:10.1016/j.lithos.2007.07.010.
- 859 McKenzie, D., 1978, Some remarks on the development of sedimentary basins: *Earth and*
860 *Planetary Science Letters*, v. 40, p. 25–32, doi:10.1016/0012-821X(78)90071-7.
- 861 McWhae, J.R.H., Elie, R., Laughton, K.C., and Gunther, P.R., 1980, Stratigraphy and
862 petroleum prospects of the Labrador Shelf: *Bulletin of Canadian Petroleum Geology*,

863 v. 28, p. 460–488.

864 Peace, A., McCaffrey, K., Imber, J., Hobbs, R., van Hunen, J., and Gerdes, K., 2015,
865 Quantifying the influence of sill intrusion on the thermal evolution of organic-rich
866 sedimentary rocks in nonvolcanic passive margins: An example from ODP 210–1276,
867 offshore Newfoundland, Canada: Basin Research, doi:10.1111/bre.12131.

868 Philippon, M., Willingshofer, E., Sokoutis, D., Corti, G., Sani, F., Bonini, M., and Cloetingh,
869 S., 2015, Slip re-orientation in oblique rifts: *Geology*, v. 43, p. 147–150,
870 doi:10.1130/G36208.1.

871 Ranero, C.R., and Pérez-Gussinyé, M., 2010, Sequential faulting explains the asymmetry and
872 extension discrepancy of conjugate margins: *Nature*, v. 468, p. 294–299,
873 doi:10.1038/nature09520.

874 Reid, I.D., and Keen, C.E., 1990, High seismic velocities associated with reflections from
875 within the lower oceanic crust near the continental margin of eastern Canada: *Earth and
876 Planetary Science Letters*, v. 99, p. 118–126, doi:10.1016/0012-821X(90)90075-9.

877 Rock, N.M.S., 1986, The nature and origin of ultramafic lamprophyres: Alnoites and allied
878 rocks: *Journal of Petrology*, v. 27, p. 155–196, doi:10.1093/petrology/27.1.155.

879 Shallaly, N.A., Beier, C., Haase, K.M., and Hamed, M.S., 2013, Petrology and
880 geochemistry of the Tertiary Suez rift volcanism, Sinai, Egypt: *Journal of Volcanology
881 and Geothermal Research*, v. 267, p. 119–137, doi:10.1016/j.jvolgeores.2013.10.005.

882 Smith, W.H., and Sandwell, D., 1997, Global sea floor topography from satellite altimetry
883 and ship depth soundings: *Science*, v. 277, p. 1956–1962,
884 doi:10.1126/science.277.5334.1956.

885 Srivastava, S.P., 1978, Evolution of the Labrador Sea and its bearing on the early evolution of
886 the North Atlantic: *Geophysical Journal International*, v. 52, p. 313–357,
887 doi:10.1111/j.1365-246X.1978.tb04235.x.

- 888 Srivastava, S.P., and Roest, W.R., 1999, Extent of oceanic crust in the Labrador Sea: Marine
889 and Petroleum Geology, v. 16, p. 65–84, doi:10.1016/S0264-8172(98)00041-5.
- 890 Shipboard Scientific Party, 1987, Site 646, *in* Srivastava, S.P., et al., Proceedings of the
891 Ocean Drilling Program, Initial reports, Volume 105: College Station, Texas, Ocean
892 Drilling Program, p. 419–674, doi:10.2973/odp.proc.ir.105.104.1987.
- 893 Storey, M., Duncan, R.A., Pedersen, A.K., Larsen, L.M., and Larsen, H.C., 1998, $^{40}\text{Ar}/^{39}\text{Ar}$
894 geochronology of the West Greenland Tertiary volcanic province: Earth and Planetary
895 Science Letters, v. 160, p. 569–586, doi:10.1016/S0012-821X(98)00112-5.
- 896 Tappe, S., Foley, S.F., Jenner, G.A., Heaman, L.M., Kjarsgaard, B.A., Romer, R.L., Stracke,
897 A., Joyce, N., and Hoefs, J., 2006, Genesis of ultramafic lamprophyres and carbonatites
898 at Aillik Bay, Labrador: A consequence of incipient lithospheric thinning beneath the
899 North Atlantic Craton: Journal of Petrology, v. 47, p. 1261–1315,
900 doi:10.1093/petrology/egl008.
- 901 Tappe, S., Foley, S.F., Stracke, A., Romer, R.L., Kjarsgaard, B.A., Heaman, L.M., and Joyce,
902 N., 2007, Craton reactivation on the Labrador Sea margins: $^{40}\text{Ar}/^{39}\text{Ar}$ age and Sr-Nd-Hf-
903 Pb isotope constraints from alkaline and carbonatite intrusives: Earth and Planetary
904 Science Letters, v. 256, p. 433–454, doi:10.1016/j.epsl.2007.01.036.
- 905 Tappe, S., Steenfelt, A., Heaman, L.M., and Simonetti, A., 2009, The newly discovered
906 Jurassic Tikiusaaq carbonatite-aillikite occurrence, West Greenland, and some remarks
907 on carbonatite-kimberlite relationships: Lithos, v. 112, p. 385–399,
908 doi:10.1016/j.lithos.2009.03.002.
- 909 Torske, T., and Prestvik, T., 1991, Mesozoic detachment faulting between Greenland and
910 Norway: Inferences from Jan Mayen fracture zone system and associated alkalic
911 volcanic rocks: Geology, v. 19, p. 481–484, doi:10.1130/0091-
912 7613(1991)019<0481:MDFBGA>2.3.CO;2.

- 913 Umpleby, D., 1979, Geology of the Labrador Shelf: Geological Survey of Canada Paper 79-
 914 13, 34 p.
- 915 Wardle, R.J., et al., 2002, Correlation chart of the Proterozoic assembly of the northeastern
 916 Canadian-Greenland Shield: Canadian Journal of Earth Sciences, v. 39, 895,
 917 doi:10.1139/e01-088.
- 918 Welford, J.K., and Hall, J., 2007, Crustal structure of the Newfoundland rifted continental
 919 margin from constrained 3-D gravity inversion: Geophysical Journal International,
 920 v. 171, p. 890–908, doi:10.1111/j.1365-246X.2007.03549.x.
- 921 Welford, J.K., and Hall, J., 2013, Lithospheric structure of the Labrador Sea from constrained
 922 3-D gravity inversion: Geophysical Journal International, v. 195, p. 767–784,
 923 doi:10.1093/gji/ggt296.
- 924 Wernicke, B., 1985, Uniform-sense normal simple shear of the continental lithosphere:
 925 Canadian Journal of Earth Sciences, v. 22, p. 108–125, doi:10.1139/e85-009.
- 926 White, J.D.L., and Ross, P.S., 2011, Maar-diatreme volcanoes: A review: Journal of
 927 Volcanology and Geothermal Research, v. 201, p. 1–29,
 928 doi:10.1016/j.jvolgeores.2011.01.010.
- 929 White, R.S., 1992, Magmatism during and after continental break-up, *in* Storey, B.C., et al.,
 930 eds., Magmatism and the Causes of Continental Break-up: Geological Society of London
 931 Special Publication 68, p. 1–16, doi:10.1144/GSL.SP.1992.068.01.01.
- 932 Whittaker, J.M., Goncharov, A., Williams, S.E., Müller, R.D., and Leitchenkov, G., 2013,
 933 Global sediment thickness data set updated for the Australian-Antarctic Southern Ocean:
 934 Geochemistry, Geophysics, Geosystems, v. 14, p. 3297–3305, doi:10.1002/ggge.20181.
- 935 Wilson, R.W., Klint, K.E.S., Van Gool, J.A.M., McCaffrey, K.J.W., Holdsworth, R.E., and
 936 Chalmers, J.A., 2006, Faults and fractures in central West Greenland: Onshore
 937 expression of continental break-up and sea-floor spreading in the Labrador–Baffin Bay

938 Sea: Geological Survey of Denmark and Greenland Bulletin 11, p. 185–204,
 939 [http://www.geus.dk/DK/publications/geol-survey-dk-gl-bull/11/Documents/nr11_p185-](http://www.geus.dk/DK/publications/geol-survey-dk-gl-bull/11/Documents/nr11_p185-204.pdf)
 940 204.pdf.

941 Wilton, D.H.C., Taylor, R.C., Sylvester, P.J., and Penney, G.T., 2002, A review of
 942 kimberlitic and ultramafic lamprophyre intrusives from northern Labrador, *in* Current
 943 Research: Newfoundland Department of Mines and Energy Geological Survey Report
 944 02-1, p. 343–352.

945 Woolley, A.R., Bergman, S.C., Edgar, A.D., Le Bas, M.J., Mitchell, R.H., Rock, N.M.S., and
 946 Scott Smith, B.H., 1996, Classification of lamprophyres, lamproites, kimberlites, and the
 947 kalsilitic, melilitic, and leucitic rocks: *Canadian Mineralogist*, v. 34, p. 175–186.

948 **FIGURE CAPTIONS**

949 Figure 1. (A) Summary of documented occurrences of early rift-related (Triassic–Cretaceous)
 950 magmatism on the margins of the Labrador Sea, both onshore and in offshore wells. ODP—
 951 Ocean Drilling Program. (B) Interpretation of the age and structure of oceanic crust in the
 952 Labrador Sea (modified from Srivastava and Roest, 1999). Abbreviations: SFZ—Snorri
 953 fracture zone; CFZ—Cartwright fracture zone; JFZ—Julinhaab fracture zone; MFZ—Minna
 954 fracture zone. The bathymetry data are from Smith and Sandwell (1997; global topography
 955 and bathymetry).

956 Figure 2. Simplified tectonic framework of central Labrador modified from LaFlamme et al.
 957 (2013), including the location of Figure 3 within the Makkovik Province. Abbreviations:
 958 NAC—North Atlantic Craton; BZ—Border Zone; GZ/JB—Granite Zone/Julianehåb
 959 Batholith; NP—Nain Province; MP—Makkovik Province; PsZ—Psammite Zone; PeZ—
 960 Peliet Zone; SECP—southeastern Churchill Province; KD—Kaipokok Domain; AD—Ailik
 961 Domain; GV—Grenville Province; KMB—Ketilidian Mobile Belt. Inset: The correlation of
 962 the Makkovik and Ketilidian orogenic belts modified from Kerr et al. (1997).

963 Figure 3. Map of the area surrounding Makkovik. Blue filled boxes depict the samples
 964 collected and analyzed in this study. The Tappe et al. (2007) samples are depicted as smaller
 965 red and green boxes, for sites visited and not visited by this study, respectively.

966 Figure 4. (A) Looking west onto the location AP1 in which three dike samples were analyzed
 967 during the study (AP1-S1, AP1-S2, AP1-S3). (B) Looking southeast.

968 Figure 5. (A) An overview of occurrences of diatreme breccia in Ford's Bight along with the
 969 locations of samples collected during this study and Tappe et al. (2007). For the location of
 970 the samples on this inset within Ford's Bight, see Figure 3. Differentiation is made between a
 971 green diatreme breccia that resembles AP2-S5 (green cross) and one that is more yellow in
 972 color, similar to AP2-S6 (yellow cross). Many of the occurrences shown are not in situ. (B)
 973 The spatial relationship between the different lithologies described at AP2. (C) Looking
 974 southeast onto the two small (<50 cm) crosscutting melilitite dikes (samples AP2-S1 and
 975 AP2-S2) within the Ford's Bight diatreme. (D) The contact between dike 1 (sample AP1-S1)
 976 and the surrounding diatreme breccia (sample AP2-S5) looking toward the south. (E) Boulder
 977 on the beach in Ford's Bight looking west comprising green diatreme breccia (similar to
 978 AP2-S5) but with an exceptionally large inclusion of mafic igneous material. (F) Possible in
 979 situ outcrop similar to sample AP2-S6 in Ford's Bight looking west. In C and D, purple and
 980 red outlines are used to denote the contacts of the dikes from which the samples AP2-S1 and
 981 AP2-S2, respectively, were obtained with the breccia and the metamorphosed basement. The
 982 blue line in C and D is the contact between the breccia and the basement, whereas the dashed
 983 white line represents the boundary between the quartzite basement and an amphibolite dike
 984 also forming part of the basement. The orange and yellow stars in B, C, and D are located at
 985 the same point for reference between these subfigures.

986 Figure 6. (A) An overview looking north of the area surrounding the global positioning
 987 system (GPS) location of ST253 in Tappe et al. (2007) taken from the location of the in situ

988 dike shown in C. (B) Looking north onto out of situ boulders in the gully 70 m away from
989 ST253. Two rock types of boulders were present in this gully: (1) granite and (2) olivine
990 clinopyroxenite. Our sample AP3-S1 is olivine clinopyroxenite. (C) A relatively good
991 exposure of in situ dike 120 m away on a bearing of 170° from AP2-ST253, which may have
992 been part of the dike contributing to the boulders in the gully.

993 Figure 7. Looking northwest from the location of sample ST254. A good exposure of the
994 Cape Strawberry Granite was observed at ST254, but no nephelinite dikes were observed at
995 this location. This is the location of the only sample $^{40}\text{Ar}/^{39}\text{Ar}$ dated by Tappe et al. (2007), to
996 which the rest of the Early Cretaceous nephelinite suite is tied.

997 Figure 8. (A) Looking north toward a bridge structure in a small dike (sample AP4-S1)
998 observed 15 m south of the global positioning system location of ST245. (B) 17 m away from
999 ST245 looking down (north up) onto the other dike observed at this location (sample AP4-
1000 S2). (C) Looking east onto location AP4 depicting dikes from which samples AP4-S1 (yellow
1001 outline) and AP4-S2 (red outline) were obtained. The dike from which sample AP4-S2 was
1002 obtained also contains a bridge structure.

1003 Figure 9. (A) Stereonet of poles to planes for the dike contacts at the sample localities. (B)
1004 Rose diagram using 5° bins of the dike contacts using the mean value of each dike contact
1005 data set plotted alongside the margin orientation (130° and 150°) derived using the modern
1006 coastline on satellite imagery.

1007 Figure 10. Thin section micrographs in both plane and cross-polarized light for all the
1008 samples described herein.

1009 Figure 11. Total alkalis versus silica plot (Le Bas et al., 1986) depicting the dike samples
1010 collected and analyzed by this study along with the Early Cretaceous nephelinite suite of
1011 Tappe et al. (2007). Samples of the same color represent the same location.

1012 Figure 12. (A) Bathymetry of the Labrador Sea from Smith and Sandwell (1997) data;
1013 mbsf—meters below seafloor. (B) Bathymetric transects along profiles 1, 2, and 3. (C) Total
1014 sedimentary thickness in the Labrador Sea from the National Oceanic and Atmospheric
1015 Administration world's oceans and marginal seas total sedimentary thickness (version 2;
1016 Whittaker et al., 2013). (D) Total sedimentary thickness transects along profiles 1, 2, and 3.
1017 For C and D, the Labrador end of the transect is at the left (0 km) and the West Greenland
1018 end is on the right. Profiles 1, 2, and 3 approximately correspond to the seismic reflection
1019 lines BGR77–17, BGR77–21, and BGR77–12, respectively. The profiles used in this study
1020 have been extended along the same trajectory as their corresponding seismic to the present
1021 coastline, thus allowing us to study the full width of the continental shelf.

1022 Figure 13. Segments of the two-dimensional seismic reflection profiles 90-R3 and 90-R1 for
1023 the Labrador and southwest Greenland margins, respectively, with interpretations of the base
1024 postrift and base synrift. The location of these segments is depicted in Figure 1.

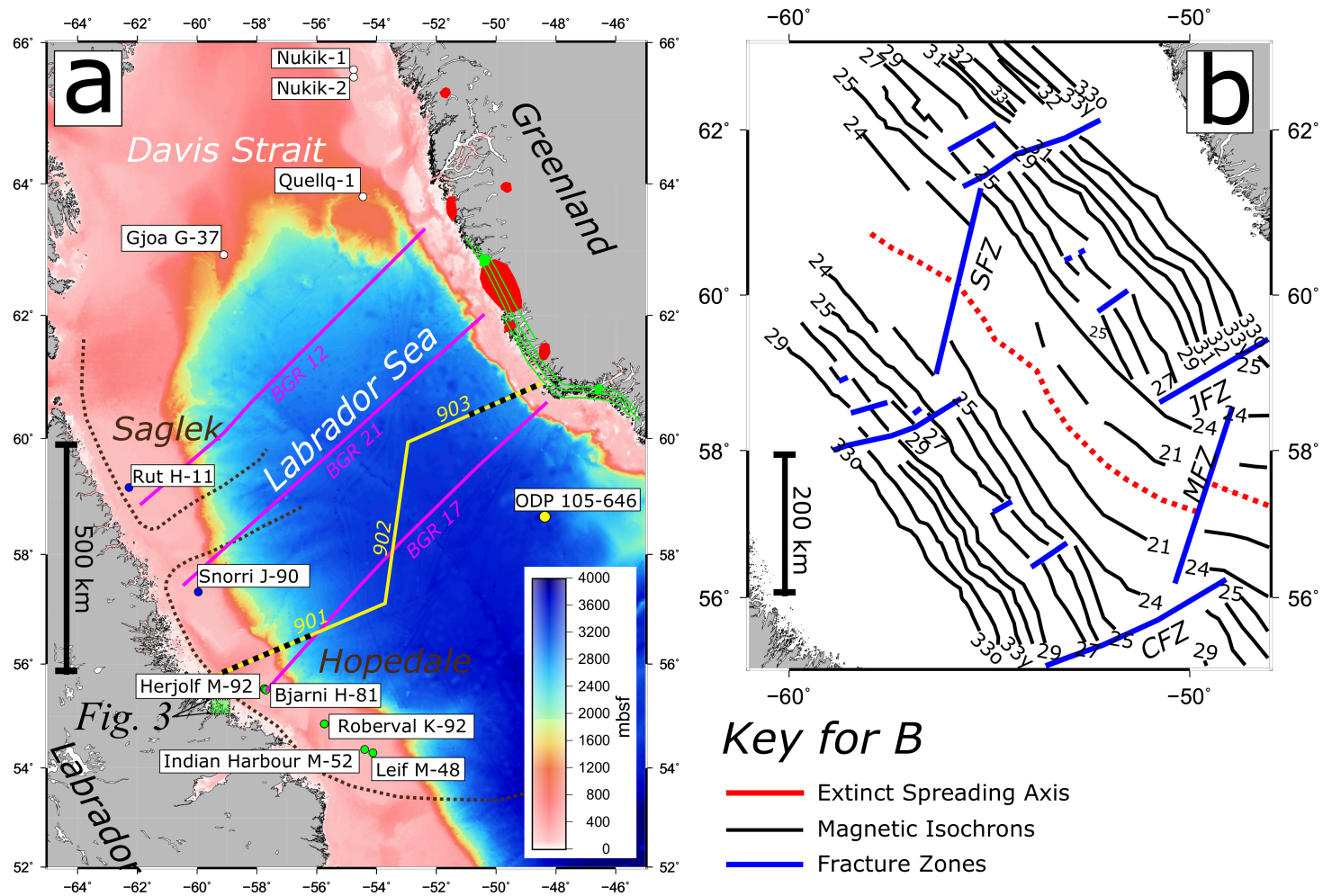
1025 Figure 14. Velocity structure of the margins of the Labrador Sea reconstructed to polarity
1026 chron C27 (Danian) reproduced from Chian et al. (1995b). OBS—ocean bottom seismograph.

1027 Figure 15. Total alkalies versus silica plot (Le Bas et al., 1986) depicting the dike samples
1028 collected and analyzed by this study along with the Early Cretaceous magmatic suite near
1029 Makkovik (Tappe et al., 2007), the Rio Grande Rift, Yarmony Mountain lavas (Leat et al.,
1030 1990), the Suez Rift (Shallaly et al., 2013), and the Central Atlantic Magmatic Province
1031 (CAMP) in Algarve, southern Portugal (Martins et al., 2008) along with Guyana and Guinea
1032 (Deckart et al., 2005).

1033 Figure 16. (A) Conceptual model of early continental rifting prior to the opening of the
1034 Labrador Sea under a simple shear rifting regime. (B) Conceptual model of late continental
1035 rifting. (C) Schematic depiction of the post-breakup (present) architecture of the conjugate
1036 passive margins of the Labrador Sea showing the preserved architecture from the early

1037 simple shear rifting modified from Lister et al. (1986), including the wide and narrow
1038 continental shelves for the Labrador and Greenland margins, respectively, the deep
1039 sedimentary basins offshore Labrador, and the minimal offshore sedimentary cover and
1040 elevated passive margin on the Greenland side of the rift. (D) The theoretical distribution of
1041 melt volumes against proximity to the rift axis where the region of melting is offset from the
1042 rift axis due to the simple shear-type early rifting. The three documented rift-related
1043 magmatic events included in green in A and D are (1) Early Cretaceous nephelinite dikes
1044 near Makkovik (Tappe et al., 2007); (2) the offshore Labrador volcanics (Umpleby, 1979);
1045 and (3) the coast-parallel dikes onshore southwest Greenland (Larsen et al., 2009). (E)
1046 Enlarged section off inset C in this figure showing the theoretical basin geometries on the
1047 upper plate Labrador margin.

Figure 1



Key for A

- West Greenland Jurassic & Triassic Intrusions - Larsen et al., (2009)
- West Greenland Cretaceous Intrusions - Larsen et al., (2009)
- Labrador Early Cretaceous Intrusive Suite - Tappe et al., (2007)
- Labrador Shelf well containing Alexis Formation Volcanics
- Labrador Shelf well containing non-Alexis Formation Volcanics
- Davis Strait well containing Paleogene Basalts
- ODP well
- Sedimentary Basin offshore Labrador
- Select lines from BGR-77 survey
- Seismic lines 901, 902 and 903
- Sections used on Fig. 5

Key for B

- Extinct Spreading Axis
- Magnetic Isochrons
- Fracture Zones

Figure 2

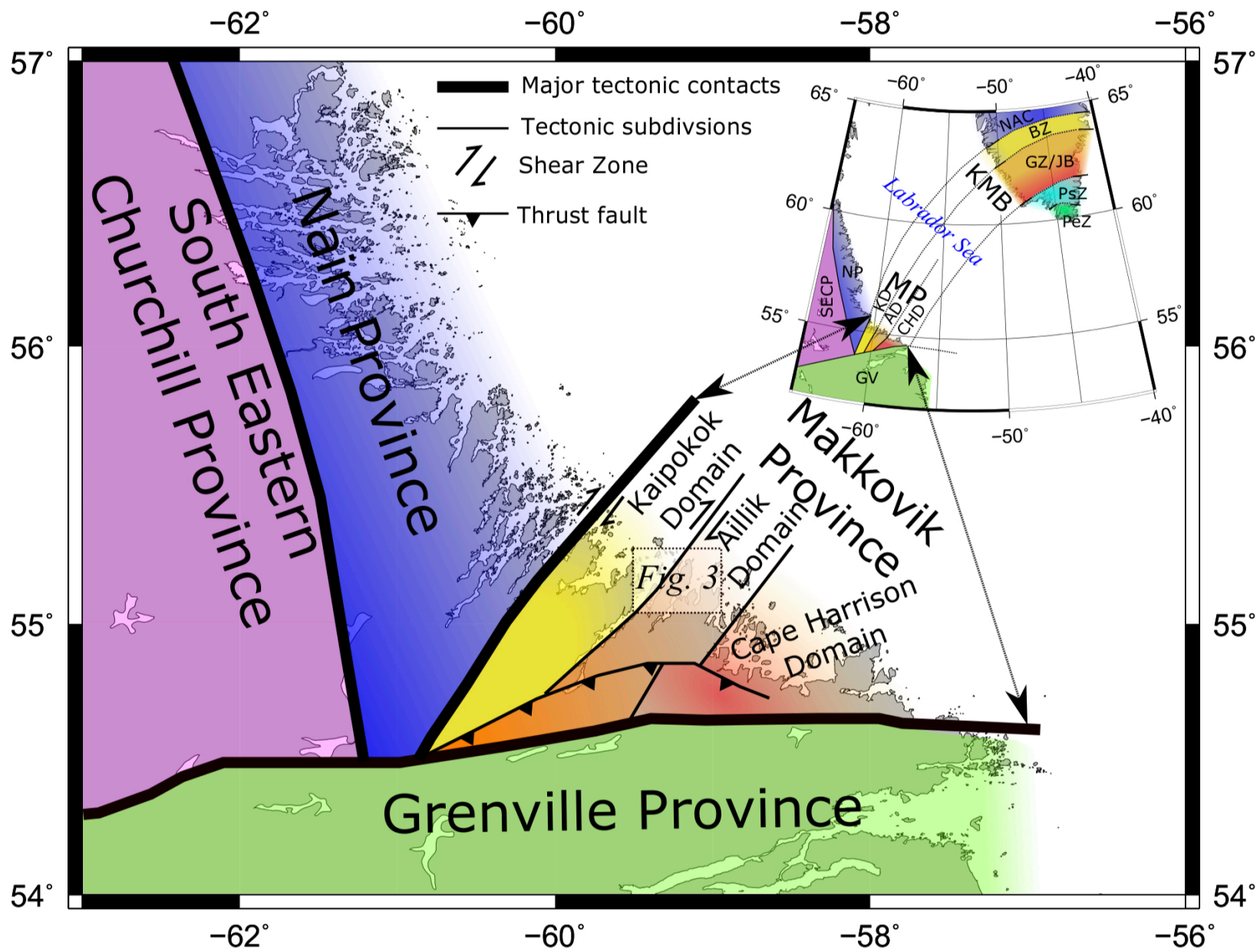


Figure 3

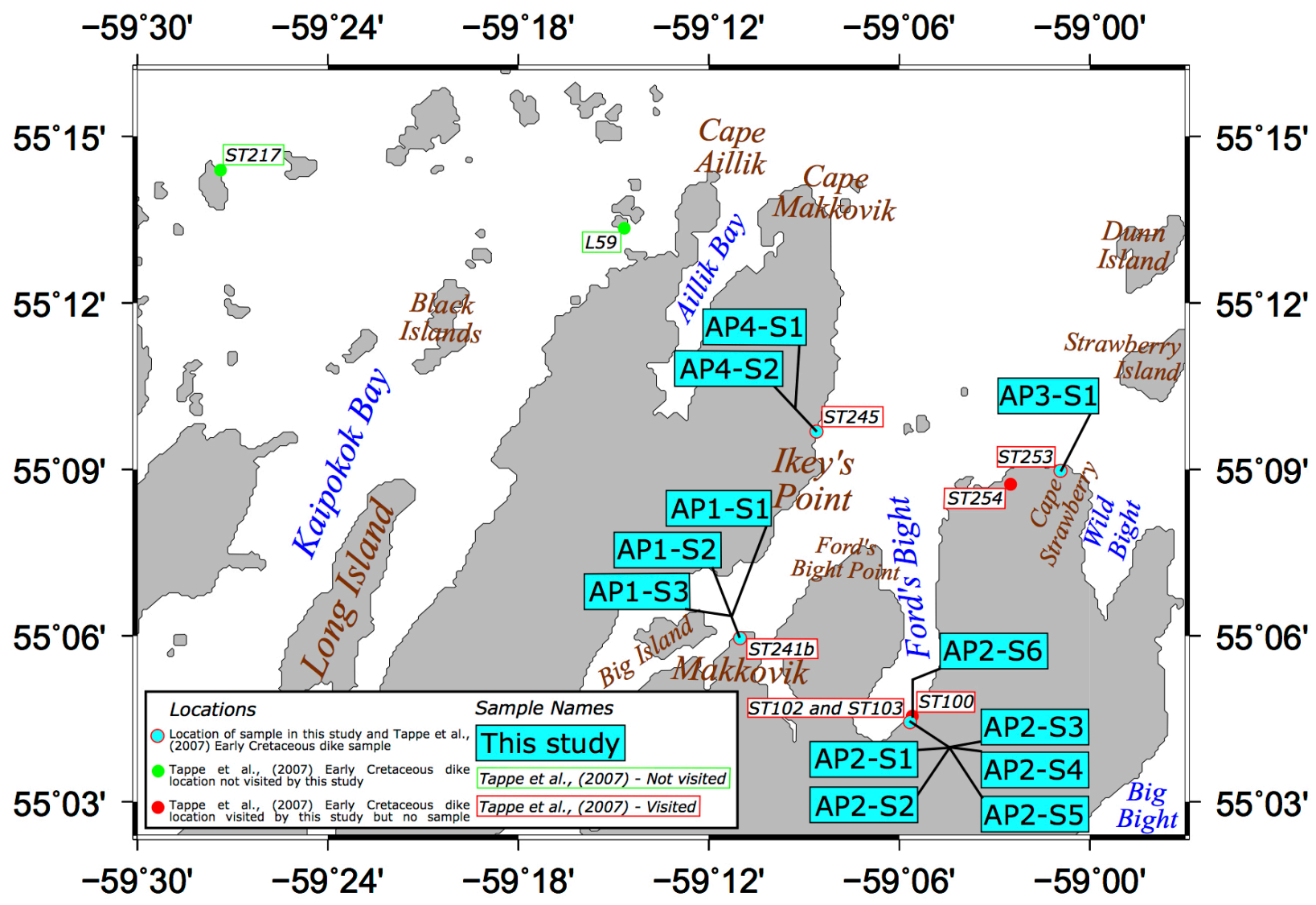


Figure 4

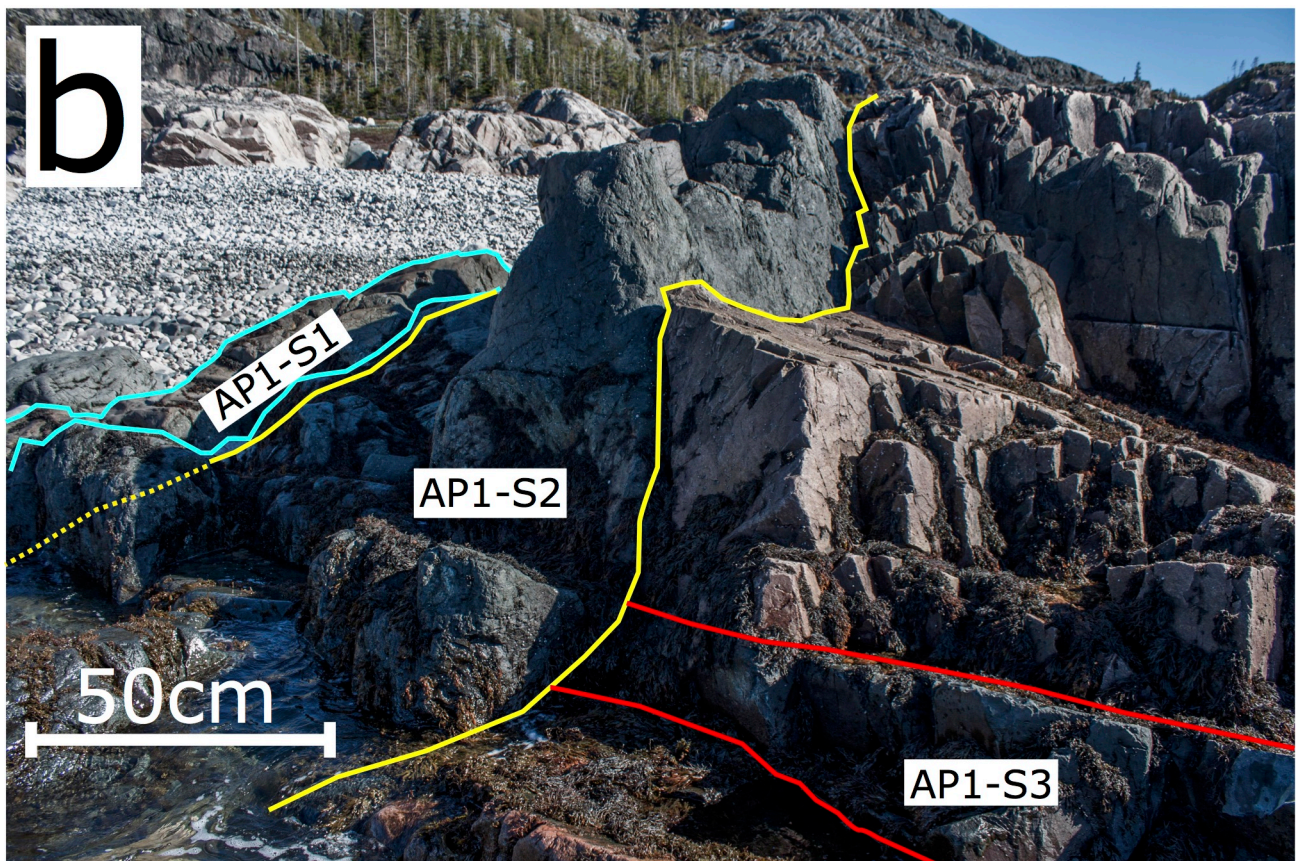
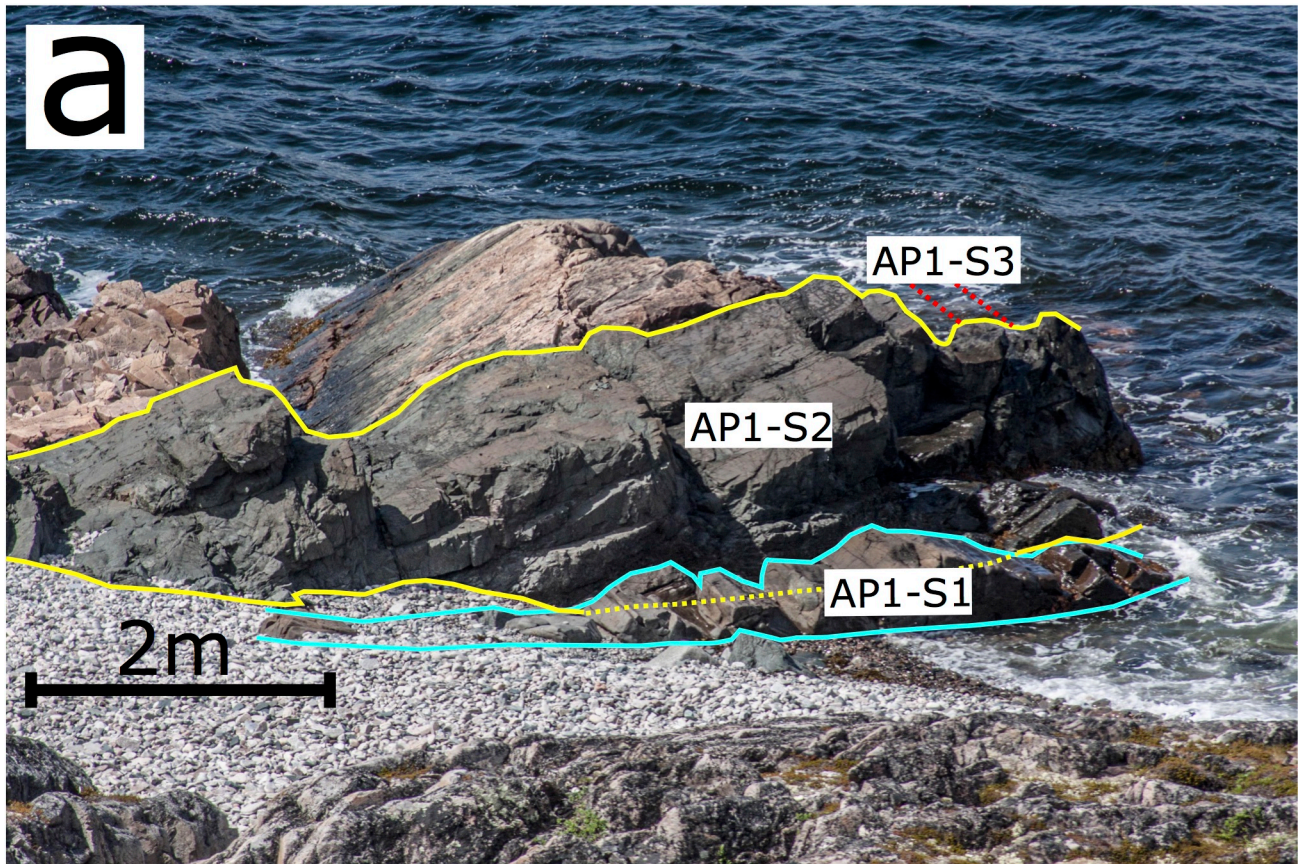


Figure 5

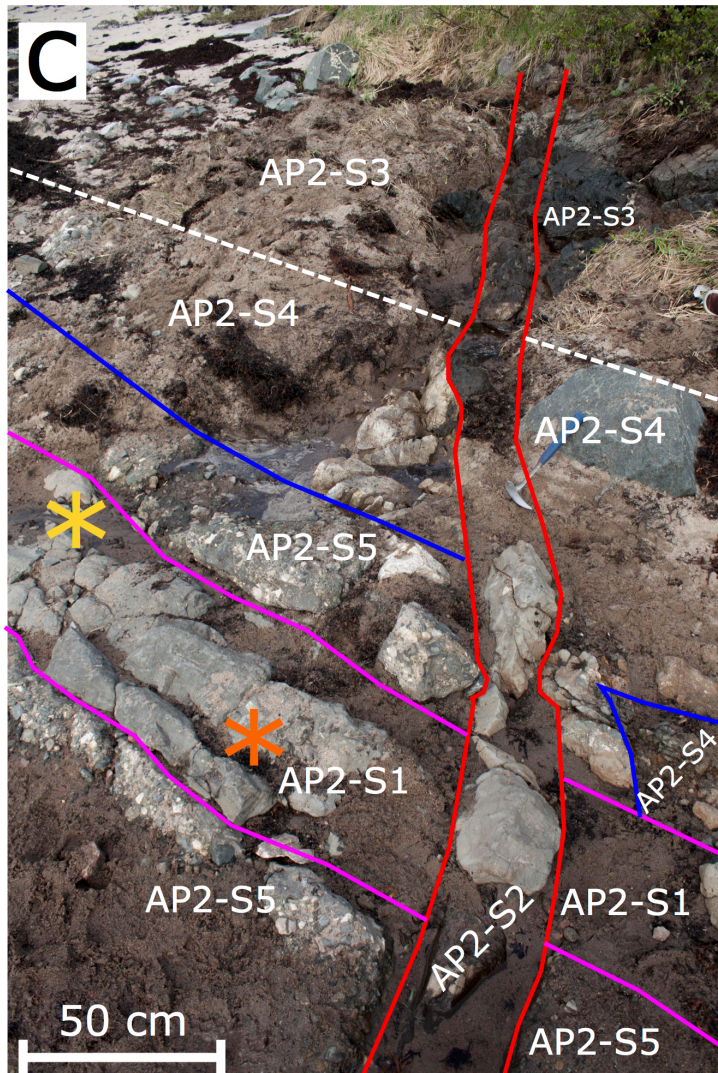
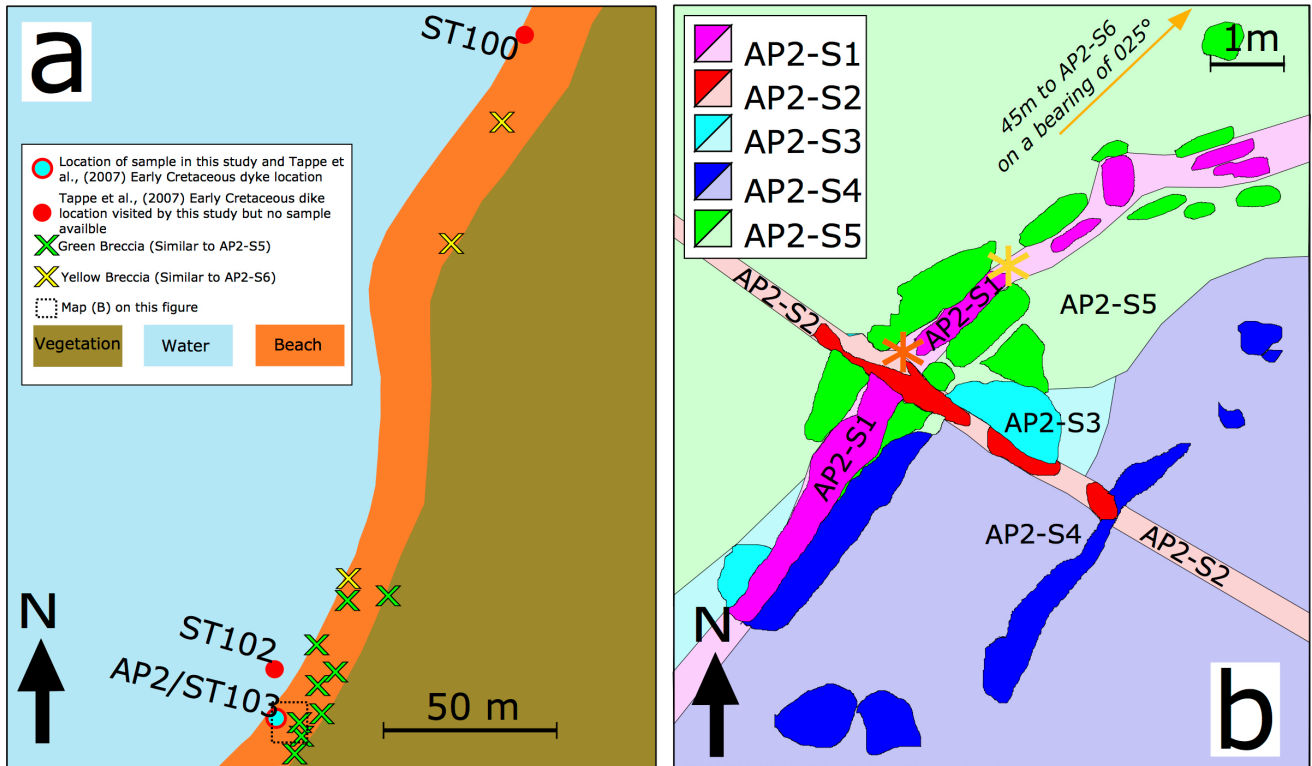


Figure 6

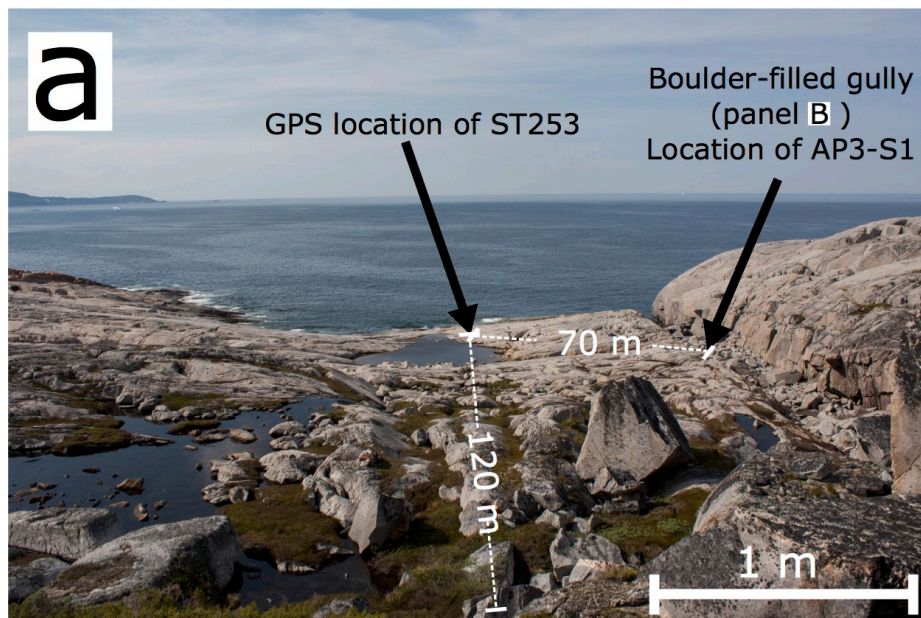


Figure 7



Figure 8

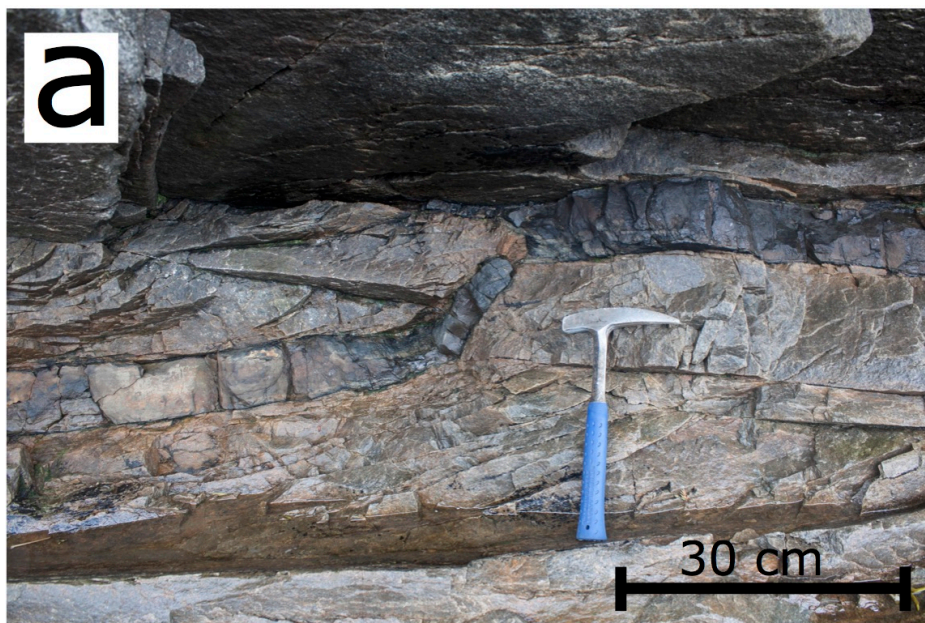
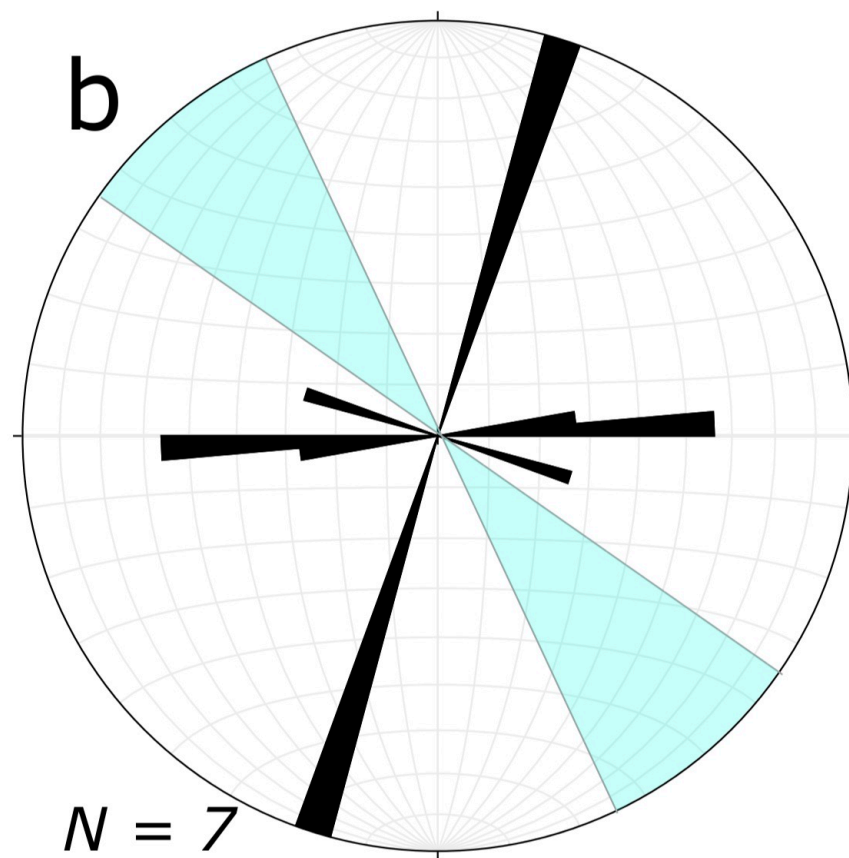
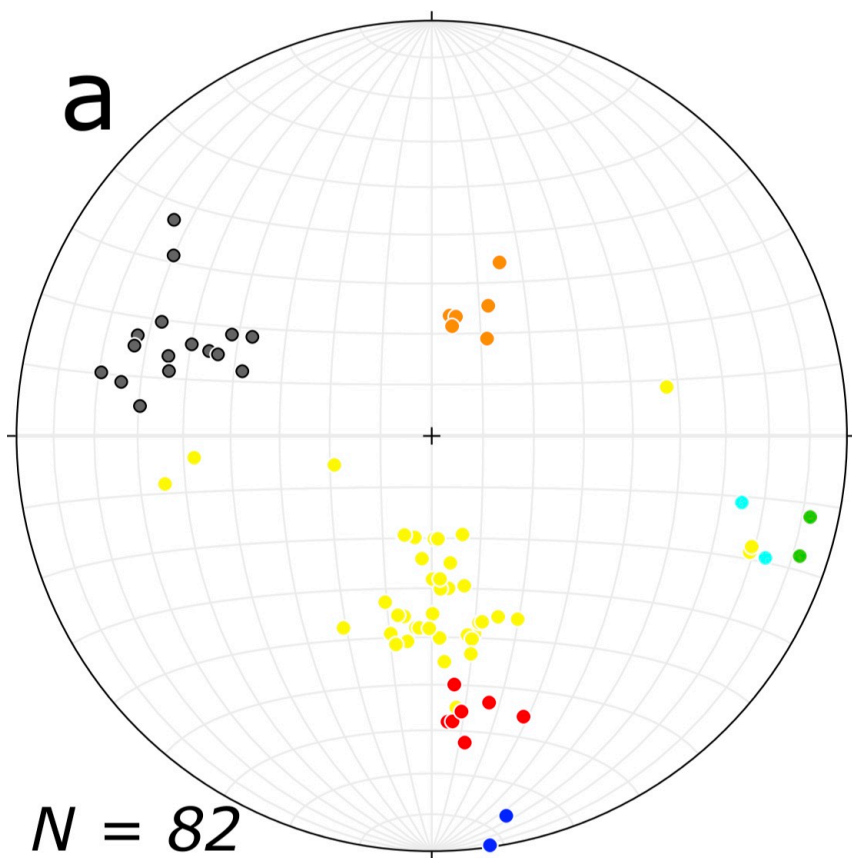


Figure 9



AP1-S1



AP1-S3



AP2-S2



AP4-S2



AP1-S2



AP2-S1



AP4-S1



Margin Orientation



Figure 10

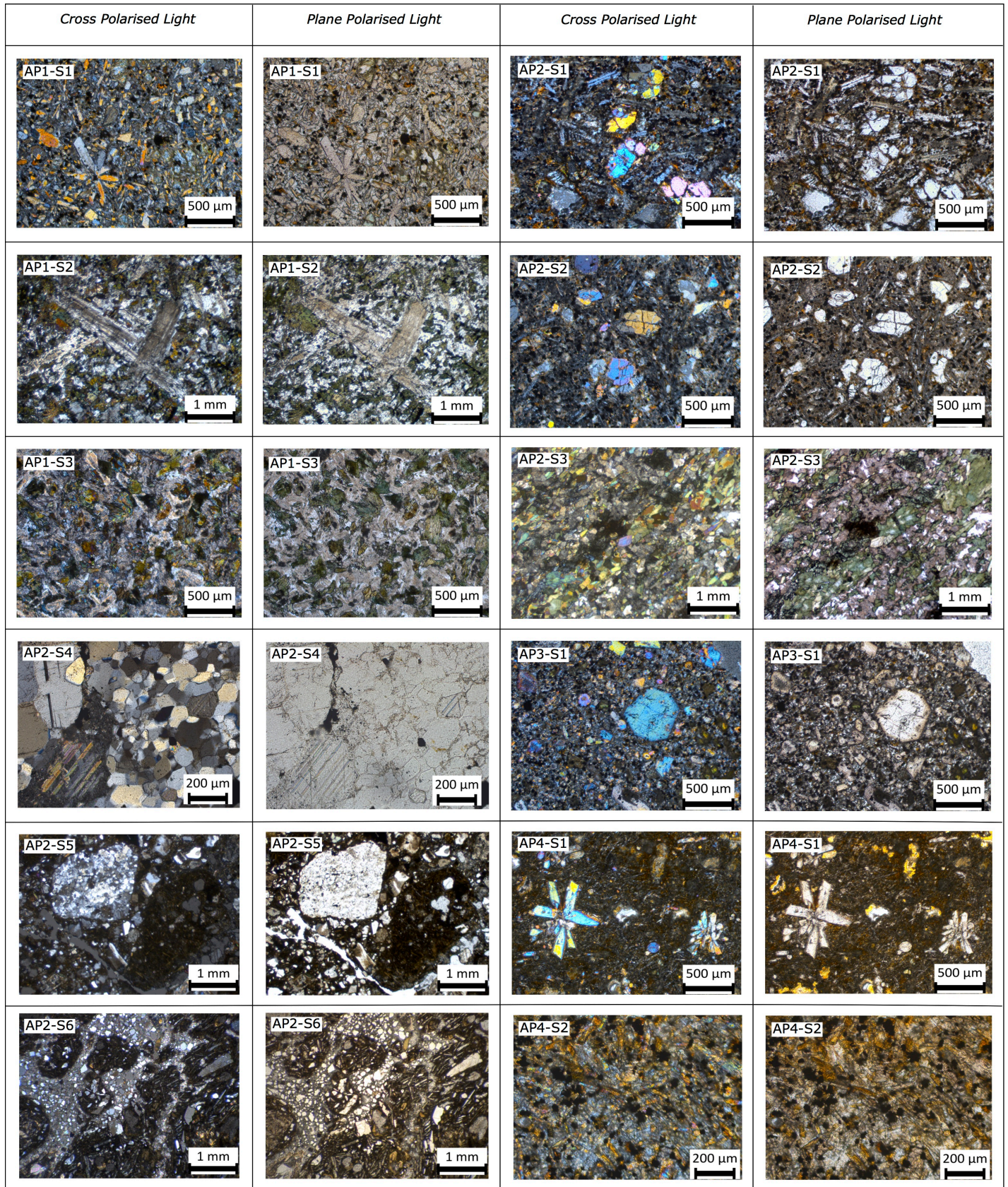


Figure 11

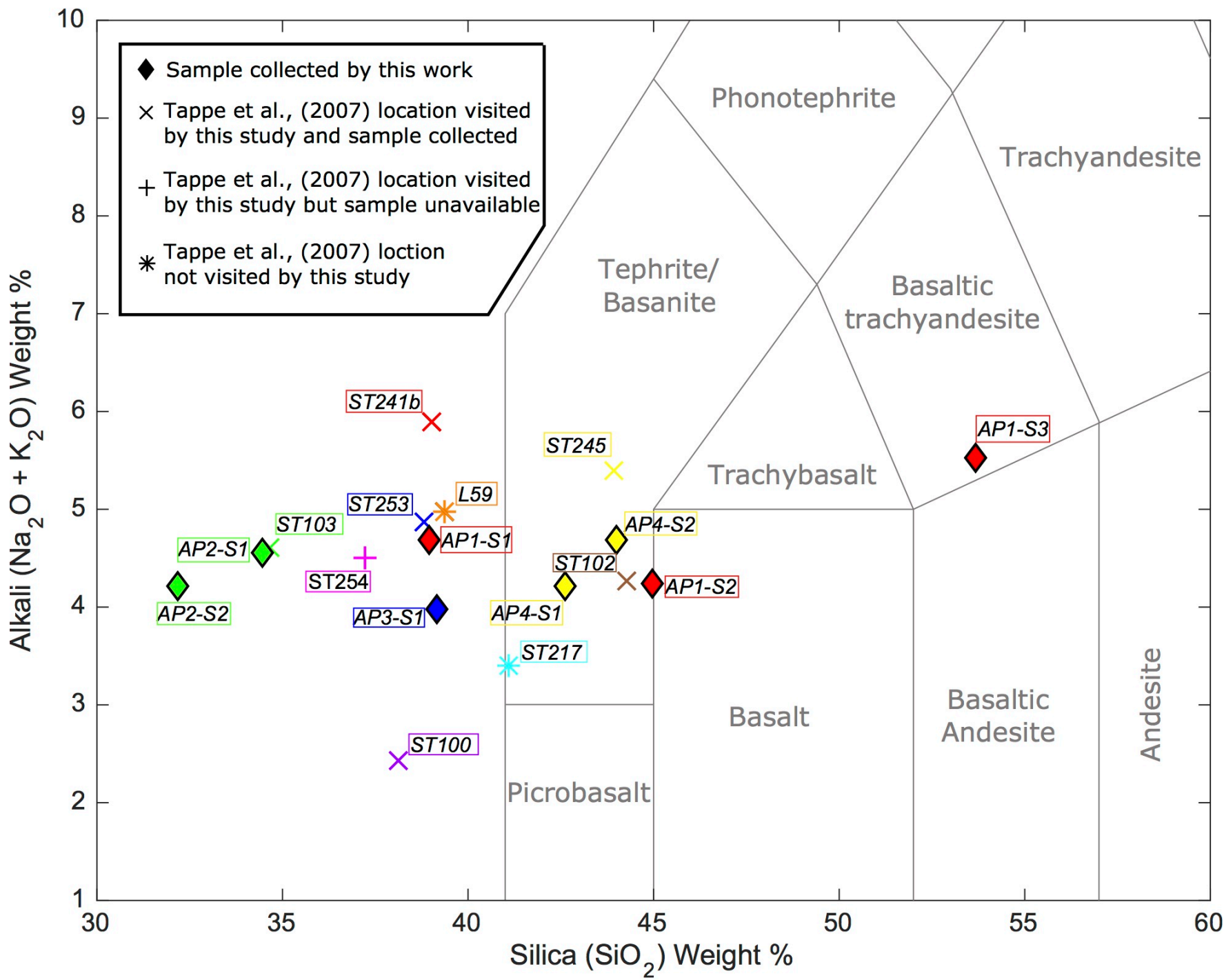


Figure 12

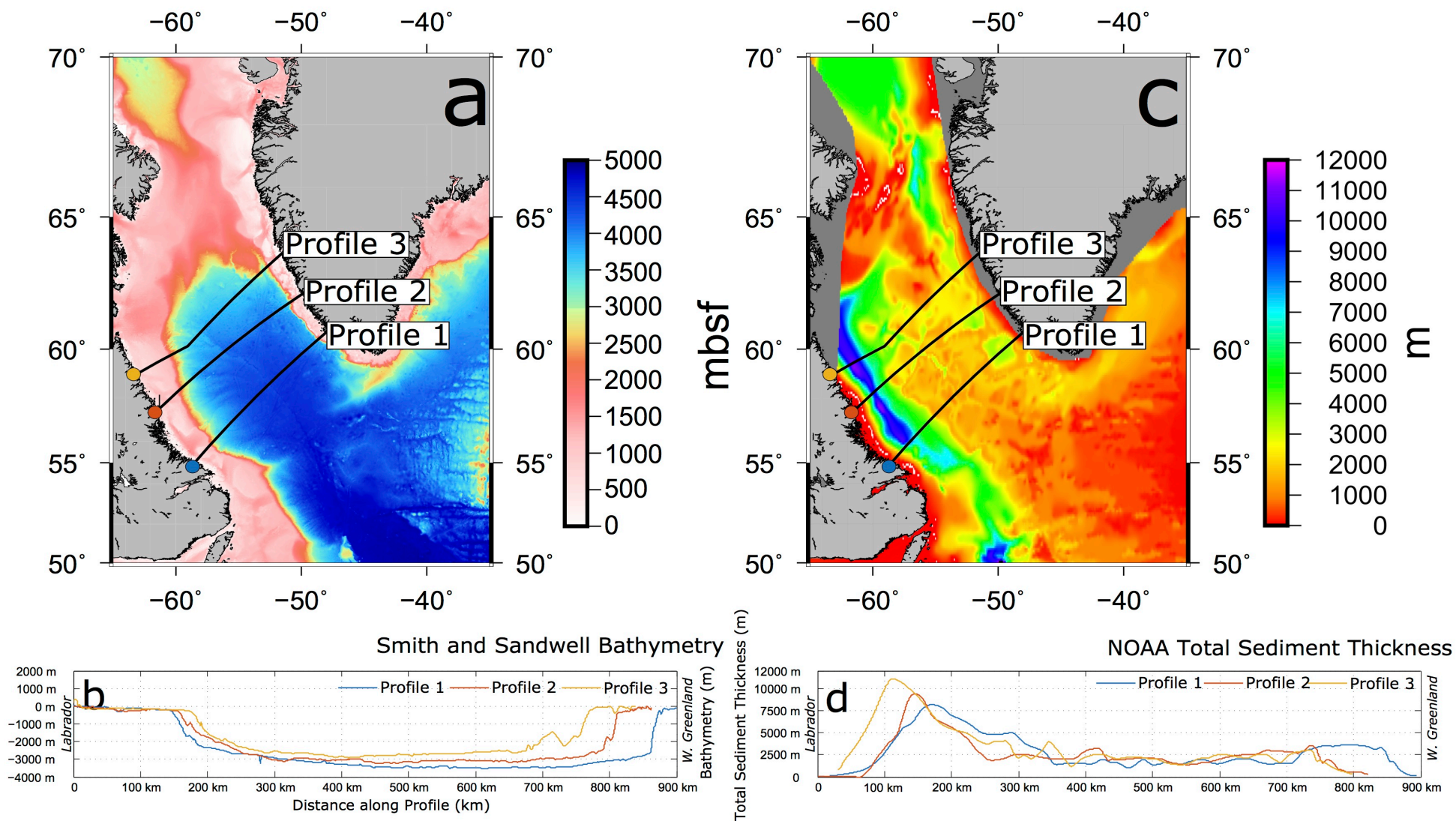


Figure 13

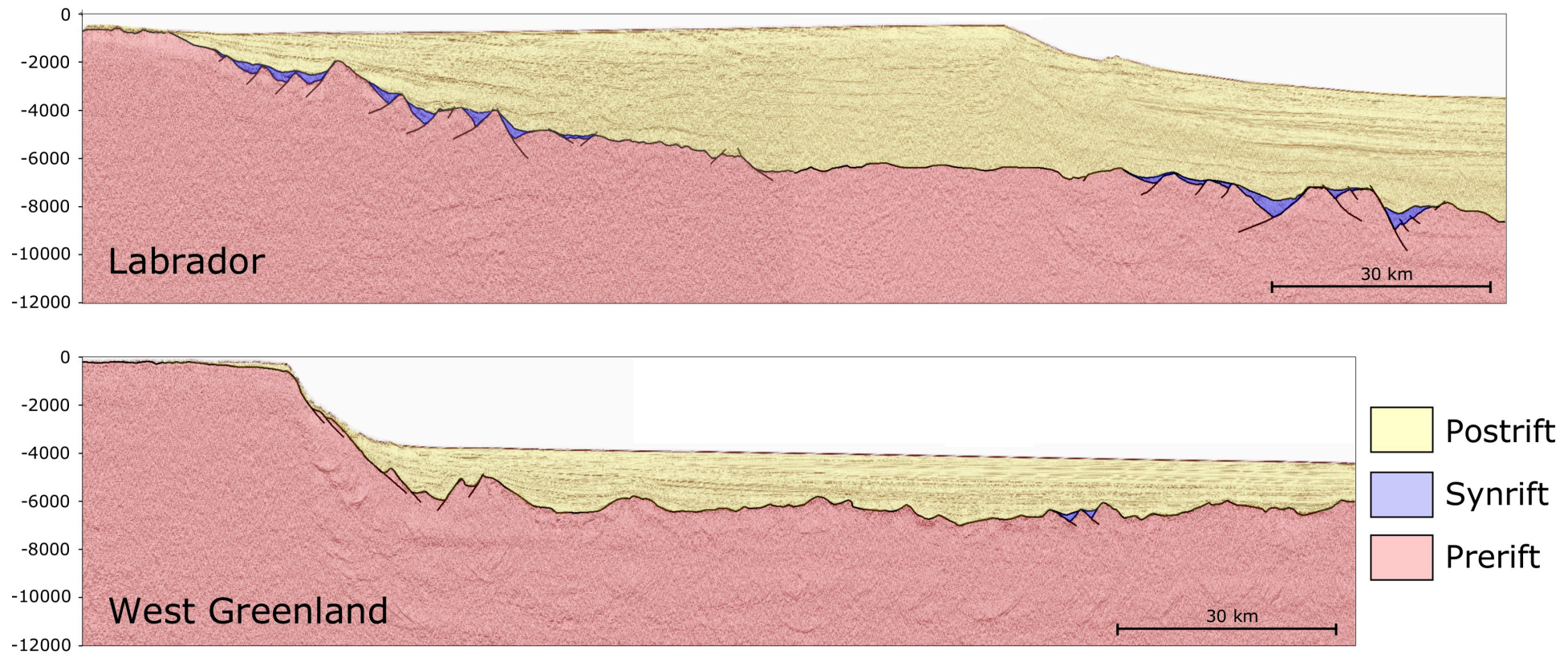


Figure 14

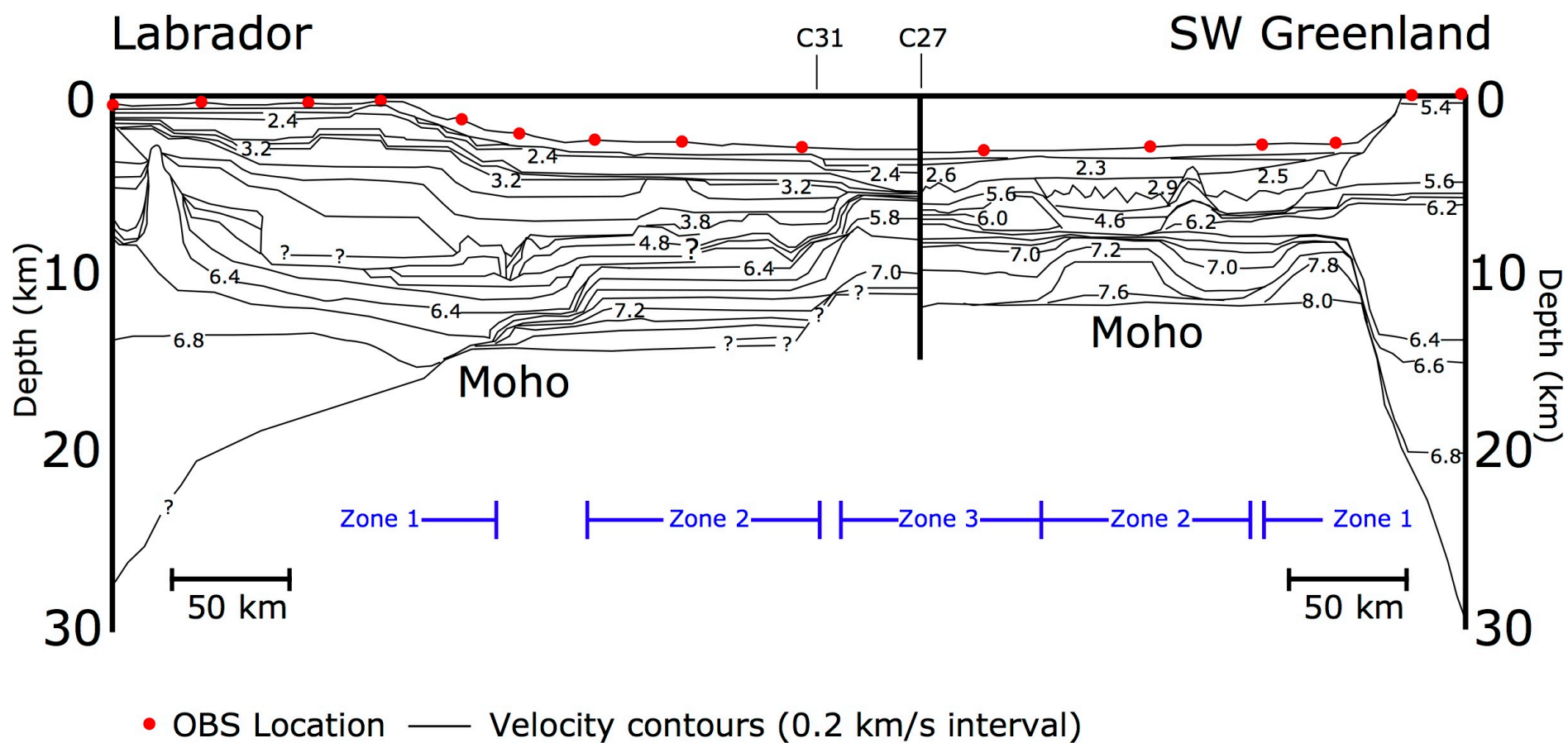


Figure 15

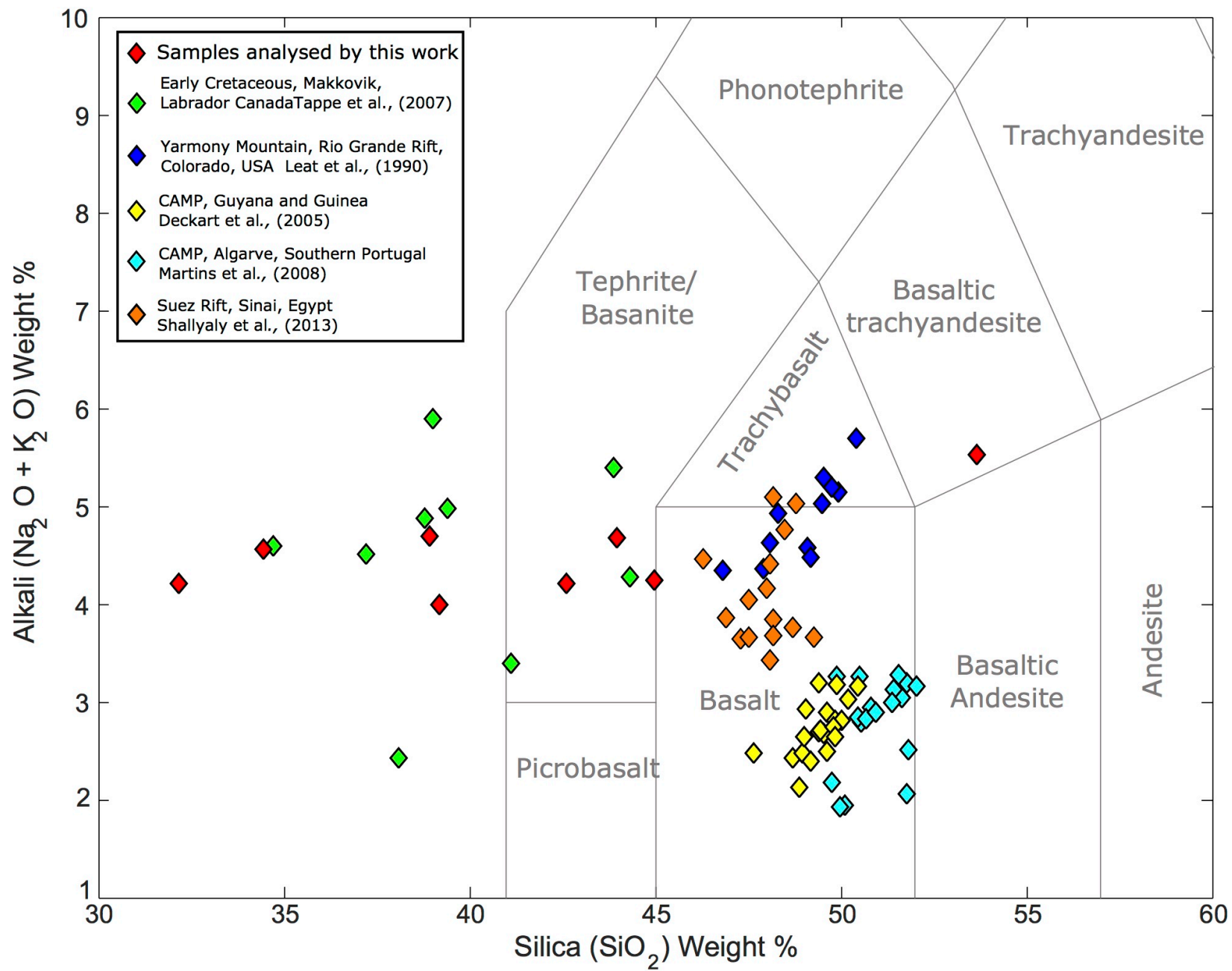


Figure 16

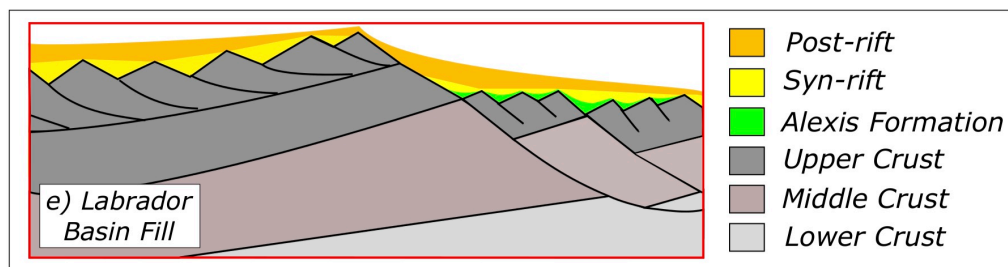
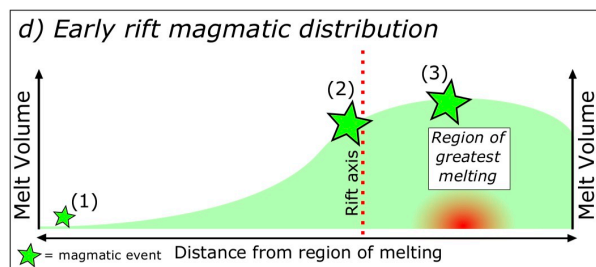
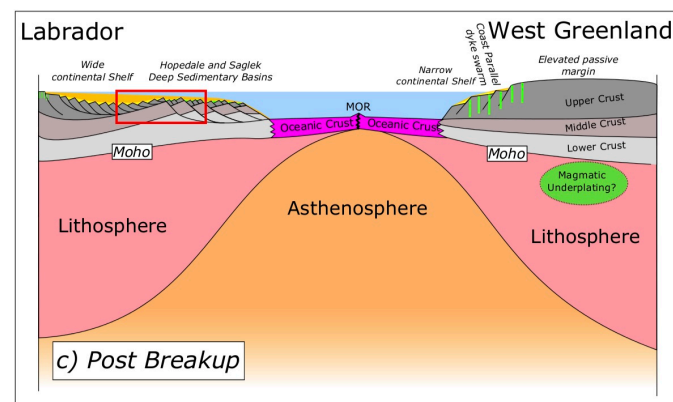
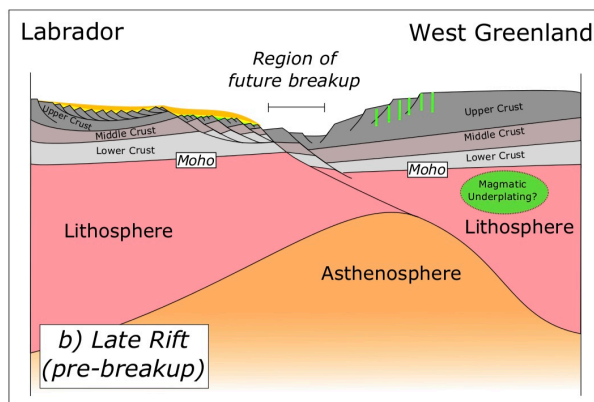
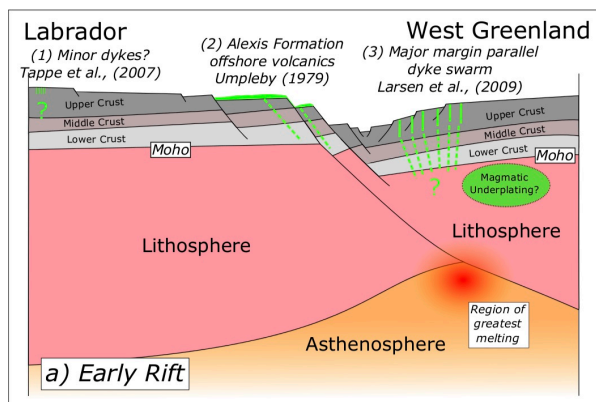


TABLE 1. SUMMARY OF RELATIONSHIP BETWEEN EARLY CRETACEOUS NEPHELINITE SUITE SAMPLES OF TAPPE ET AL. (2007), AND SAMPLES COLLECTED FOR THIS WORK

Tappe et al. (2007) sample number	ST100	ST102	ST241b	L59	ST217	ST103	ST253	ST245	ST254
Composition (Tappe et al., 2007)	Nephelinite	Basanite	Nephelinite	Nephelinite	Basanite	Melilitite	Nephelinite	Basanite	Nephelinite
Samples collected by this work (AP)	No in situ outcrop at location	No in situ outcrop at location	AP1-S1 AP1-S2 AP1-S3	Not visited in our study	Not visited in our study	AP2-S1 AP2-S2	AP3-S1	AP4-S1 AP4-S2	Area of basement exposure but no dikes of any age anywhere in proximity to location.
Coordinates of samples collected by this work (WGS84)	n/a	n/a	55.09927N 59.18356W	n/a	n/a	55.07389N 59.09430W	55.14959N 59.01542W	55.16138N 59.14338W	n/a

Note: WGS84—World Geodetic System 1984. n/a—not applicable as no equivalent sample was obtained by this work.

TABLE 2. DOCUMENTED OCCURANCES OF RIFT RELATED MAGMATISM IN SOUTHWEST GREENLAND

Locality	Character	Rock type	Method	Age (Ma)	Reference
Uummannaq Fjord	Few small dikes	aillikite	Rb-Sr	186	Larsen et al. (2009)
Ubekendt Eiland	Small dike swarm	camptonite, monchiquite	$^{40}\text{Ar}/^{39}\text{Ar}$	34 ± 0.2	Storey et al. (1998)
Southeast Nuussuaq	Dikes and sill, some large	tholeiitic basalt	$^{40}\text{Ar}/^{39}\text{Ar}$	56.8 ± 0.2	Larsen et al. (2009)
West of Disko	Volcanic neck	alkali basalt	$^{40}\text{Ar}/^{39}\text{Ar}$	27.8 ± 0.6	Storey et al. (1998)
Western Disko	Regional dike swarm	tholeiitic basalt	$^{40}\text{Ar}/^{39}\text{Ar}$	54.3 ± 0.3	Storey et al. (1998)
Aasiaat district	Three large dikes , one sill	tholeiitic basalt	$^{40}\text{Ar}/^{39}\text{Ar}$	56, 61	Larsen et al. (2009)
Itilleq	One dike	tholeiitic basalt	$^{40}\text{Ar}/^{39}\text{Ar}$	64 ± 1.3	Larsen et al. (2009)
Qaqqarsuk	Central complex and dikes	carbonatite, aillikite	Rb-Sr U-Pb*	ca. 165	Secher et al. (2009)
Fossilik	One explosion breccia	aillikite	Rb-Sr	164.2 ± 1.8	Secher et al. (2009)
Søndre Isortoq	Small dike swarm	camptonite, one alkali basalt	$^{40}\text{Ar}/^{39}\text{Ar}$	56, 58	Larsen et al. (2009)
Godthåbsfjord	Scattered dikes	camptonite	$^{40}\text{Ar}/^{39}\text{Ar}$	51.8 ± 0.9	Larsen et al. (2009)
Tikusaaq	Central complex and dikes	carbonatite and aillikite	Rb-Sr U-Pb*	165–155	Tappe et al. (2009)
Færingehavn	Few dikes	aillikite	Rb-Sr U-Pb	159 223	Larsen et al. (2009)
Frederikshåb Isblink	One large dike	phonolite	$^{40}\text{Ar}/^{39}\text{Ar}$	106.1 ± 1.5	Larsen et al. (2009)
Frederikshåb Isblink	Loose dike swarm	monchiquite, alnöite, carbonatite	Rb-Sr U-Pb*	152–149	Larsen et al. (2009)
Paamiut	Small dike swarm	aillikite	K-Ar	166 ± 5	Larsen and Møller (1968)
Pyramidefjeld	Small dikes and sills, including a thick sheet on Midternæs (16 km NNE)	aillikite	U-Pb	152–150	Frei et al. (2008) Larsen et al. (2009)
Southwest Greenland	Large regional dike swarm	mildly alkaline basalt	$^{40}\text{Ar}/^{39}\text{Ar}$	141–133	Larsen et al. (1999) Larsen et al. (2009)
Tuttutooq	One or a few sills	camptonite	$^{40}\text{Ar}/^{39}\text{Ar}$	115.4 ± 4.7	Larsen et al. (2009)

Note: A summary from north to south of documented intrusive rift-related magmatism in West Greenland as summarized by Larsen et al. (2009).

*Samples dated by Rb-Sr or U-Pb on phlogopite or perovskite.

TABLE 3. OCCURRENCES OF VOLCANIC ROCKS IN OFFSHORE WELLS ON THE LABRADOR SHELF

Well name	Depths of igneous rocks	Dating method	Age	Description and Interpretation of igneous rocks
Bjarni H-81	2255 m—total depth	K-Ar	139 ± 7 Ma for the lower core (2510 m) 122 ± 6 Ma for the upper core (2260 m)	Basalts interspersed with sandstones and silty clays, with no pyroclastic rocks. Bjarni H-81 is the type section of the Alexis Formation.
Leif M-48	1839 m—total depth	K-Ar	104 ± 5 Ma to 131 ± 6 Ma	The Leif Basalts are deemed to be coeval and lithologically similar to those in Bjarni H-81, and thus can be considered part of the Alexis Formation.
Indian Harbour M-52	3250 m—3484 m	K-Ar	90 ± 4 Ma for rock fragments (exact stratigraphic position unknown)	The recovered rock samples are lapilli tuff deposits. The volcanic rocks in this well are noted as being lithologically very different from occurrences of the Alexis Formation elsewhere on the Labrador shelf. The lithological difference along with the younger age suggests that these rocks may not be part of the Alexis Formation.
Herjolf M-92	3751 m—4048 m	K-Ar	The top of the volcanic section has been dated as 122 ± 2 Ma, whereas the bottom is dated as 314 ± 12 Ma. This bottom section is severely altered and thus the age is likely to be unreliable.	Subaerial weathered basalt flows overlying Precambrian basement. Lithologically similar to the igneous rocks in Bjarni H-81, and thus can be considered part of the Alexis Formation.
Roberval K-92	3188 m—3544 m	n/a	undated	This is the thickest recorded section of the Alexis Formation (Ainsworth et al., 2014).
Rut H-11	Tuff top at 4432 m and Diabase intrusive 4451 m C-NLOPB (2007)	n/a	undated	Igneous rocks are noted twice in the Canada-Newfoundland and Labrador Offshore Petroleum Board (2007) report: Tuff top at 4432 m and Diabase intrusive at 4451 m.
*Snorri J-90	3150 m—3061 m (Umpleby, 1979)	palynology	Valanginian to Barremian	A series of graywackes, sands, silts, and coal beds interpreted to be derived from volcanic rocks that may be coeval with the Alexis Formation but should not be referred to as part of the Alexis Formation (McWhae et al., 1980).

Note: Summary of occurrences of volcanic rocks in offshore wells on the Labrador shelf well depths are from C-NLOPB (2007); all other data and information are from Umpleby (1979) and references therein, unless otherwise stated.

*Indicates the presence of sediments potentially derived from igneous rocks. n/a—not applicable as the sample has not been dated.

TABLE 4. X-RAY FLUORESCENCE DATA

	AP1-S1	AP1-S2	AP1-S3	AP2-S1	AP2-S2	AP3-S1	AP4-S1	AP4-S2
SiO ₂	38.93	44.96	53.66	34.43	32.17	39.19	42.62	43.98
TiO ₂	2.63	3.31	0.74	2.10	2.15	2.44	1.92	1.90
Al ₂ O ₃	12.93	13.42	17.15	10.79	10.18	12.34	14.33	14.68
Fe ₂ O ₃	13.77	16.91	9.45	11.43	12.04	12.43	12.03	11.87
MnO	0.23	0.33	0.21	0.23	0.24	0.21	0.21	0.18
MgO	8.09	5.36	4.85	10.66	10.96	9.07	6.93	8.45
CaO	11.25	6.94	5.97	16.00	14.52	13.55	10.19	9.99
Na ₂ O	2.78	3.25	3.14	2.00	2.22	2.26	2.67	2.93
K ₂ O	1.91	1.00	2.39	2.57	1.99	1.73	1.54	1.75
P ₂ O ₅	1.02	1.86	0.18	2.31	2.58	0.86	0.65	0.66
SO ₃	0.33	0.01	<0.002	0.82	1.04	0.20	0.15	0.16
CrO ₃	0.02	0.00	<0.001	0.02	0.02	0.04	0.03	0.03
NiO	0.01	0.00	0.00	0.02	0.02	0.02	0.02	0.02
LOI	5.61	2.27	1.88	5.29	8.40	5.18	6.15	2.73
Total	99.51	99.63	99.62	98.67	98.52	99.51	99.44	99.34

Note: The results of X-ray fluorescence analyses for major element oxides in the dike samples (AP prefix) collected during this study. LOI—loss on ignition.

TABLE 5. MAJOR STRUCTURAL AND MAGMATIC COMPONENTS OF THE LABRADOR AND SOUTHWEST GREENLAND MARGINS

	Labrador	Southwest Greenland
Continental shelf width (Figs. 4A, 4B)	Wide (~150 km)	Narrow (~50 km)
Maximum offshore sedimentary cover (synrift and postrift) (Figs. 12C, 12D, and Fig. 5)	~12,000 m	~3700 m
Onshore intrusive magmatism	Minor nephelinite suite proposed by Tappe et al. (2007) but disputed in this study	Summarized in Table 2
Offshore magmatism	Alexis formation and other volcanics in offshore wells (Table 3)	Unknown due to absence of offshore wells
Crustal-scale detachment faults	Possibly; inferred by the presence of distinct basin (Welford and Hall, 2013)	No